SOME INVESTIGATIONS ON CONTROL OF PV-BATTERY SYSTEMS

A DISSERTATION

SUBMITTED IN PARTIAL FULLFILLMENT OF THE REQUIREMENTS
FOR THE AWARD OF THE DEGREE
OF

MASTER OF TECHNOLOGY
IN

[POWER SYSTEM]

Submitted By:

MAYANK KUMAR
(2K20PSY12)

Under the supervision of
PROF. ALKA SINGH

ELECTRICAL ENGINEERING
DELHI TECHNOLOGICAL UNIVERSITY
(Formerly Delhi College of Engineering)
Bawana Road, Delhi-110042

MAY, 2022

M. Tech (Power Systems) **MAYANK KUMAR** **2022**

DELHI TECHNOLOGICAL UNIVERSITY
(Formerly Delhi College of Engineering)
Bawana Road, Delhi-110042

CANDIDATE'S DECLARATION

I, Mayank Kumar, Roll No. 2K20PSY12 student of M.Tech (Power System), hereby declare that the Project Dissertation titled "Some investigations on control of PV-Battery systems" which is submitted by me to Department of Electrical Engineering, Delhi Technological University, Delhi in partial fulfilment of the requirement for the award of the degree of Master of Technology, is original and not copied from any source without proper citation. This work has not previously formed the basis for the award of any Degree, Diploma Associateship, Fellowship or other similar title or recognition.

Place : Delhi
Date : 30/05/2022

MAYANK KUMAR

Department of Electrical Engineering
DELHI TECHNOLOGICAL UNIVERSITY
(Formerly Delhi College of Engineering)
Bawana Road, Delhi-110042

CERTIFICATE

I hereby certify that the Project Dissertation titled "**SOME INVESTIGATIONS ON CONTROL OF PV-BATTERY SYSTEMS**" which is Submitted by Mayank Kumar, 2K20PSY12, Electrical Engineering, Delhi Technological University, Delhi in partial fulfilment of the requirement for the award of the degree of Master of Technology, is a record of the project work carried out by the student under my supervision. To the best of my knowledge this work has not been submitted in part or full for any Degree or Diploma to this University or elsewhere.

Place : Delhi
Date : 30/05/2022

PROF.ALKA SINGH
SUPERVISOR

ABSTRACT

In this thesis, reports on the modelling and simulation of the photovoltaic systems with grid connected for three phase as well as single phase, PV integrated with battery standalone system and grid to battery system are presented. The key parameters impact of PV systems on quality of the power and power generation are carried out in this research. To generate electrical power and which is also one of the fastest growing power generation in the world PV technology is one of the biggest renewable energy resources. In this thesis the grid connected system and integration of the battery storage system with the PV is seen.

In the chapter 2 simulink model of two stage power conversion of grid connected PV for a three phase system was carried out. System output was 100kW and the effects of changes in solar irradiance and temperature, on the PV system output power, are simulated. Similarly in chapter 4 single stage single phase system was simulated.

In the chapter 3 modeling and simulation of PV-Battery storage system is carried out using the MATLAB with a system of 1kW. PV panel is connected to the DC-DC converter through the DC-AC inverter to the Point of Common Coupling (PCC). The intergration of the battery storage system with the grid is carried out in the chapter 5. Very encouraging results are yielded in the battery storage system integration with the PV system that results in counteracting the fluctuation of the PV installation and thus helping in ensuring the power supply to be maintained constant.

The great process have been made by the scientists in the study of solar power. We know that solar radiation on earth is very large. Entire consumption of the energy for all human for one year can be fulfilled by the 40 minutes of solar radiation on earth. To protect the environment, ensure sustainable economic development and to alleviate the energy crisis use of solar energy is done. Solar industry is divided into solar photovoltaic industry and solar thermal industry.

ACKNOWLEDGEMENT

This thesis without the guidance and support of some people would not have been possible. First of all I would particularly like to appreciate my thesis supervisor Professor Alka Singh. She guided me in the right direction throughout the research and her door was always opened for me. Whenever I had a trouble or doubt she was always there to resolve my doubt. Therefore I owe my deepest gratitude to my professor for all her contributions of time, her expert supervision, brilliant ideas and extensive knowledge for this subject.

This acknowledgement would not be complete without the mention of parents who were with me throughout the ups and downs of this thesis and of my life. Therefore, I would like to extend my love and gratitude to my parents for their understanding and a plethora of support has been my family for me throughout the duration of my studies.

Place : Delhi **MAYANK KUMAR**

Date : 30/05/2022

CONTENTS

List of Figures

List of Tables

CHAPTER 1: INTRODUCTION

In today's world one of the basic need is electricity which is important for economic growth and industrialization of the country. Electricity is produced by the majorly renewable and non-renewable sources. Fossil fuels, nuclear resources, coal and gas are some of the non-renewable sources of energy which are serious threat to our environment. Figure 1.1 shows the global energy consumption. To overcome this, world is moving towards the use of renewable energy sources. So among electrical power resources renewable energy resources have become more advantageous in terms of environment. Moreover there has been seen decrease in solar panel prices during last 38 years.

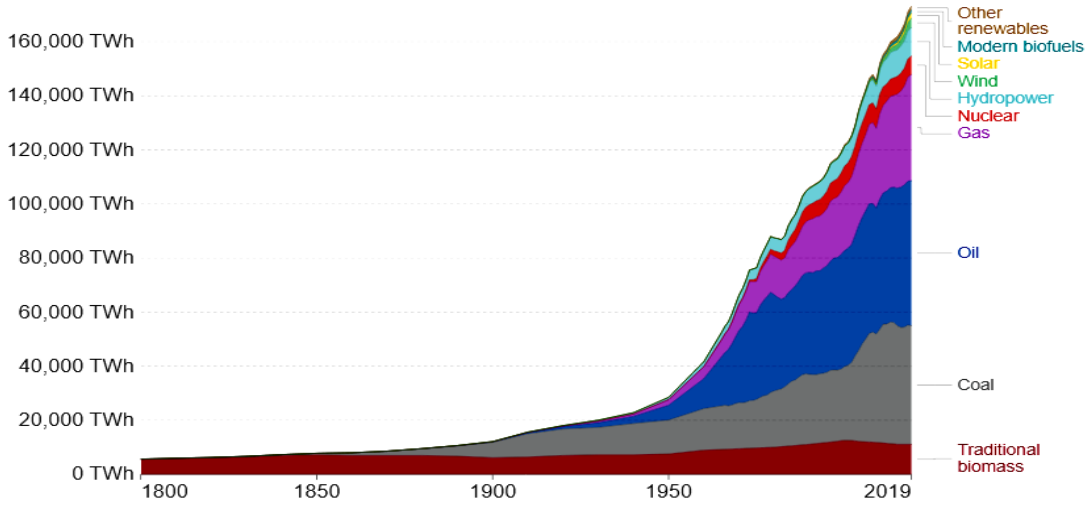

Figure 1.1 Consumption of the global energy in TW-h [1]

Solar energy is one of the important sources of energy as it is non-polluting and inexhaustible source. A PV system supplies the solar power and is composed of solar panels that convert the coming sunlight into the electrical power Due to high demand in recent years, prices of PV have declined to a considerable amount. The Indian government has established large solar farms which have the capacity to provide energy to large number of consumers [1]. PV systems can be mounted on rooftops of buildings, societies, large companies and institutions and can range from few tens of kilowatts to hundreds of kilowatts. A PV system may be grid connected or used in standalone mode of operation. The energy generated may be used by the residential consumers or commercial building. The electrical output of PV cell also depends on shading. Many methods are given in literature to compute the shading losses from trees to PV systems [3].

Two main issues are considered for the improvement of the performance of the tracking system. First, the sunlight is perpendicular to the solar panel and thus more sunlight is received as compared to the case if it were at any other angle. The second is that direct light is used more efficiently than angled light. The highest power density (170 W/m^2) among renewable energy sources is obtained from solar electric generation [3]. Ideally it is estimated that PV installations could operate for hundred years or even more with very little maintenance and capital cost. If other fossil fuel and nuclear energy resources are considered, much less amount of money is spent on the development of solar cells. Conversion efficiency of solar panel is considerably reduced by the pollen, dirt and other particulates stuck on the solar panels.

1.1 PV SYSTEMS

Since we know, the generation of photovoltaic power can only be done during daytime. The clouds can cause some unwanted fluctuations in the PV power generation output which can cause power imbalances, frequency instability and voltage imbalances. From Figure 1.2 we get to know that in 2018 globally there has been seen increase of 100GWdc of solar photovoltaic (solar PV) capacity according to the International Energy Agency (IEA). This represents the 50% more than the growth of 2015. We know consumer demand as well as the energy prices keep rising but we should thank to the monetary advantages that have been offered by state or government channels, within the India, the market for solar power equipment is on the rise.

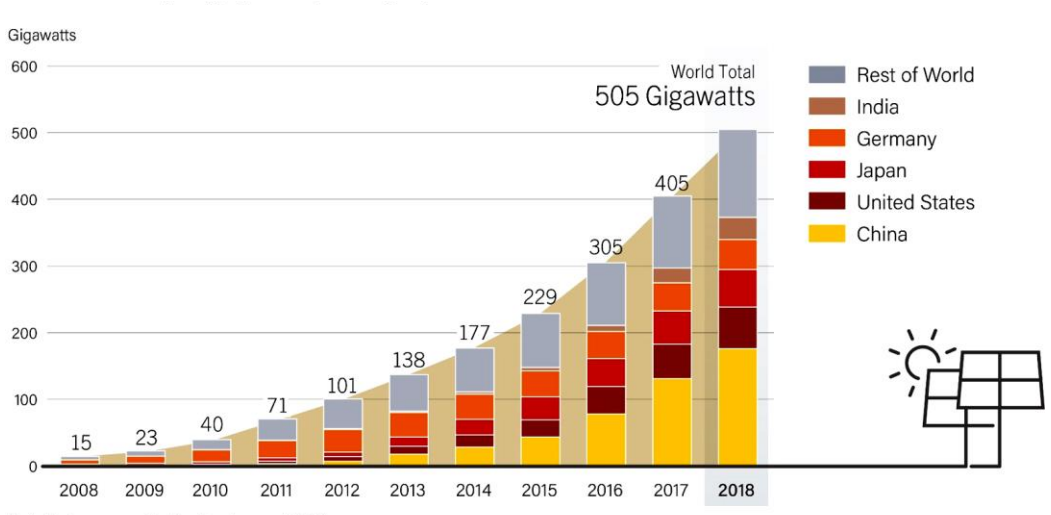

Figure 1.2 Solar PV global capacity, by country, 2008-2018 [2]

Photovoltaic (PV) systems are used for the conversion of solar energy to electricity and this photovoltaic effect was first physically observed back in 1839 in Becquerel. Electricity is produced directly from the sunlight by the photovoltaic tools through an electronic process in semiconductor materials that naturally occurs in them. PV devices are used in road signs, transportation, calculators, commercial, etc. In next 4 to 7 years a major decline of the solar PV costs as much as 50% is expected [3]. Other way by the means of an expanded capacity of manufacturing may be the interaction and learning for reducing the cost for PV. To meet a specified voltage, current and power rating, the several photovoltaic modules combination are grouped in series and parallel combinations thus forming a photovoltaic (PV) system.

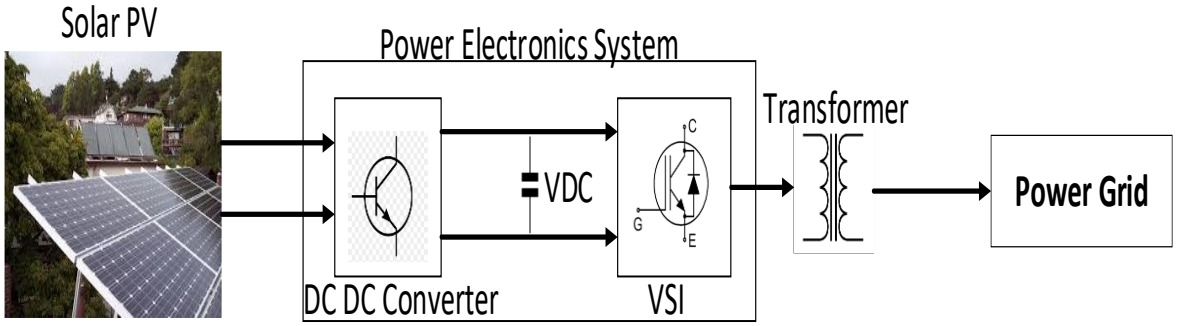

Figure 1.3 Generic structure of grid connected PV system

1.2 PV CELL

Following are the three basic attributes required for the operation of photovoltaic cell:-

i. Electron-hole pairs or excitons should be generated by the absorption of light.
ii. Charge carriers separation of opposite types.
iii. To an external circuit, those carriers should be extarcted.

Multiple solar cells forming group together in one plane forms solar PV panel or module. They are often covered with a glass sheet on the side which is sun-facing for the protection of the semiconductor material. From a solar cell to a PV system is shown in Figure 1.4. For creating the additive voltage connection of solar cells should be in series and by connecting in parallel it yields higher current.

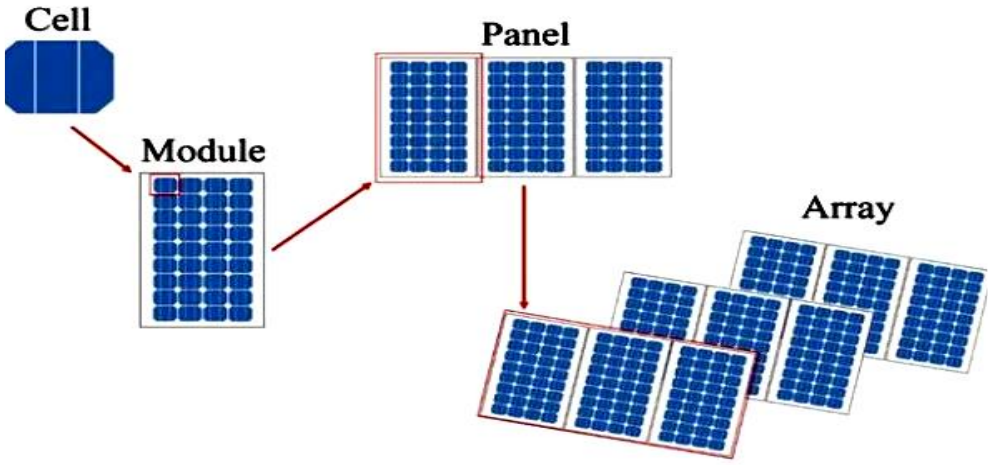

Figure 1.4 Possible components of the PV system

Various absorption and charge separation mechanisms advantage is taken by a single layer of light-absorbing material (single-junction) or multiple physical configurations (multi-junctions) that form solar cells. PV cells can be classified into three types of cells. First type are made of crystalline silicon that are made up of elements such as polysilicon and monocrystalline silicon, second type are thin film solar cells which are made up of amorphous silicon, Orgnic materials such as CdTe and CIGS are third type organometallic compounds as well as inorganic substances. According to International Renewable Energy Agency estimated the amount of 43,500-250,000 metric tons in 2016 was the solar panel electronic waste generated. The number is estimated to increase 60-78 million metric tons by 2050 [3]. There are different methods to recycle PV panels and the recycling process involves major three steps i.e. module recycling, cell recycling and waste handling. Sometimes contamination of the environment is done by the cells like CdTe as they contain toxic elements like lead and cadmium.

At the positive and negative junctions of the semiconductor free electrons and holes are created when the photons of the sunlight are absorbed by the PV cell, and then generates DC power. Basic PV cell structure can be seen in Figure 1.5. On the both sides of the cell connected are the metallic contacts that collect the power generated by the PV cells. The P-V and V-I curve that shows output of the PV cell under various operating conditions is shown in Figure 1.6 where maximum voltage and current at maximum power point is denoted by $V_{mp}I_{mp}$.

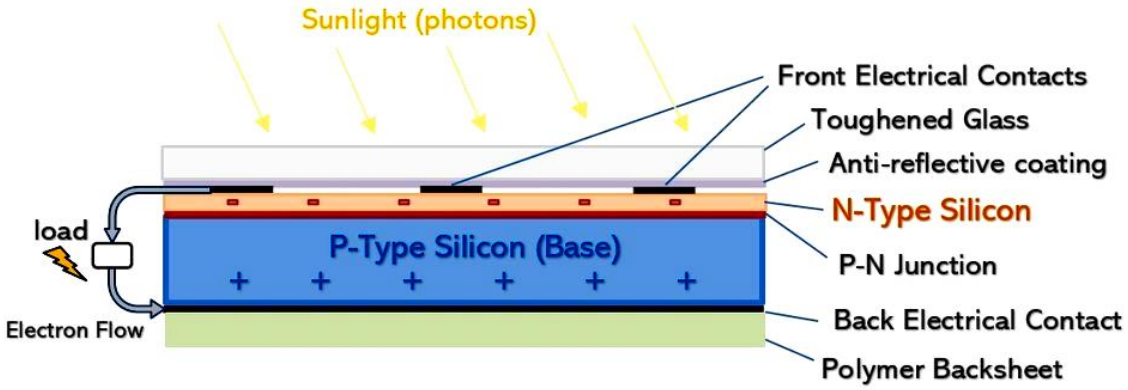

Figure 1.5 The structure of a PV cell [4]

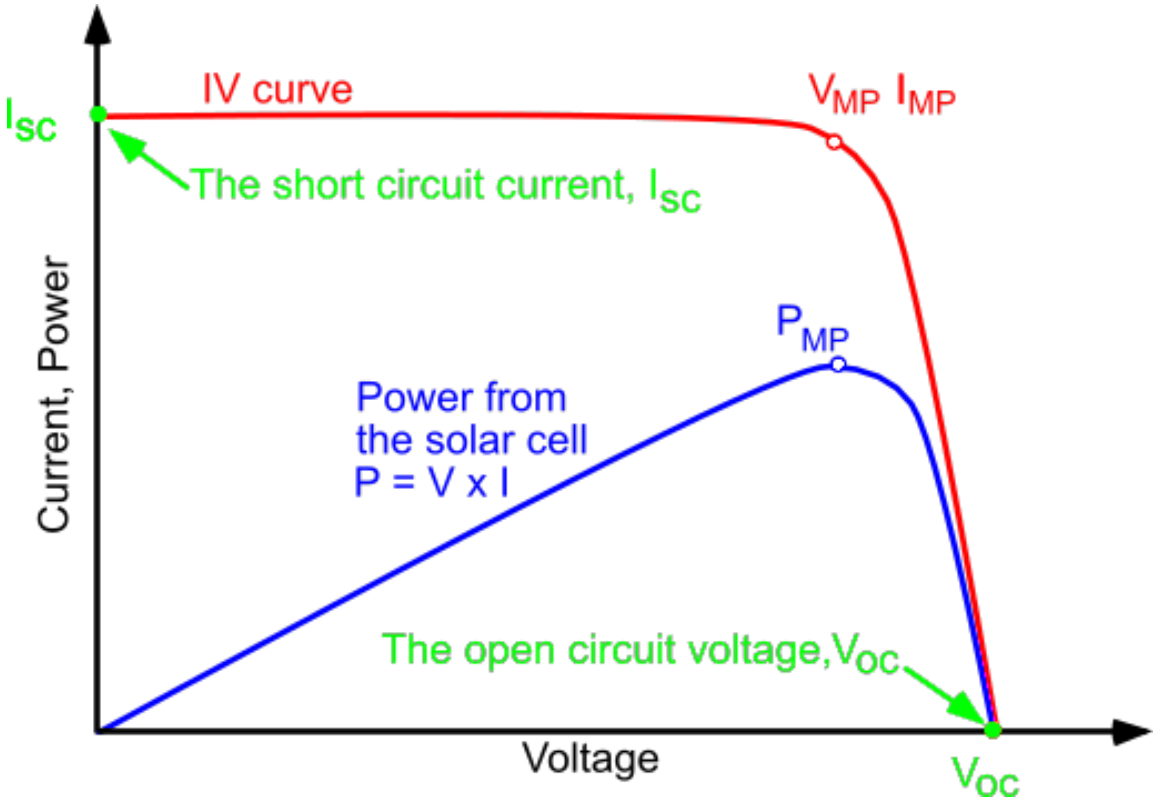

Figure 1.6 The P-V and I-V curve of a PV cell [5]

When the photovoltaic cell generates the current I it is given by the eqn.

$$I = I_L - I_O \left[exp\left(\frac{qV}{nkT}\right) - 1 \right] \quad (1.1)$$

where,

I_L = referred as short circuit current
I_O = referred as saturation current
V = referred as PV cell voltage
k = referred as Boltzmann constant
q = referred as electronic charge
T = referred as temperature

1.3 SWOT ANALYSIS OF PV SYSTEM

Table 1.1 SWOT analysis of PV system [6]

STRENGTH : 1. Installation is easy, cabling is not reqd. 2. Output is efficient, clean, renewable and non-environment polluting. 3. There is no consumption of conventional energy. 4. It is a onetime investment for whole life.	WEAKNESS : 1. Cost is high. 2. Sunlight is affected by the weather. 3. Conversion rate is low. 4. Need larger area for installation.
OPPORTUNITY : 1. Expectation of market is very broad. 2. Support of national policy made by the government. 3. Technological and scientific progress is expected.	THREATS : 1. Fluctuations in prices of the product and demand for subsidy. 2. Grid initiative.

1.4 EFFECT OF TEMPERATURE AND IRRADIANCE ON PV CELL

The factors such as temperature and irradiance affects the performance of a PV cell. We can see PV cell maintaining the linear relationship between the short circuit current and the irradiance i.e. increase or decrease in irradiance will directly affect the increase and decrease in short circuit current.

$$I_{SC}(G) = \left(\frac{G}{G_O}\right).I_{SC}G_O \tag{1.2}$$

where,

G_O = referred to irradiance reference level
G = referred to PV cell's incident irradiation

Small increase in open circuit current is seen after increasing the temperature due to narrow bandgap but decrease of the short circuit voltage takes place significantly. The dependency of PV cell on temperature is given as

$$I_{SC}(T) = I_{SCREF} + 0.006\frac{A}{K}(T - T_{REF}) \tag{1.3}$$

Also on the temperature, dependency of open circuit voltage is expressed as

$$V_{OC}(T) = \frac{E_{GO}}{q} - \frac{kT}{q} - ln\left(\frac{BT^{\gamma}}{I_{SC}}\right) \tag{1.4}$$

where,

B = constant and temperature independent
E_{GO} = linearly extrapolated zero temperature bandgap energy of the semiconductor
γ = temperature dependent

Nowadays, the renewable energy sources that is most promising nowadays, the PV system are seen in street lightning, water pumping, home applications, large scale power plants, supplying telecommunication transmitters, vehicle applications, space applications, etc. Connection with directly to the grid of the PV modules, is not possible.

The performance of the PV cell is measured by the one of the most important parameter and also measures the quality of the junction is called fill factor and is given by,

$$F_F = \frac{V_{mp} I_{mp}}{V_{OC} I_{SC}} \tag{1.5}$$

Solar's cell ideal fill factor value is 1 which means the PV cell is highest quality. The parasitic elements of a PV cell decreases the fill factor value. The circuit representation of parasitic elements in PV cell is shown in Figure 1.7.

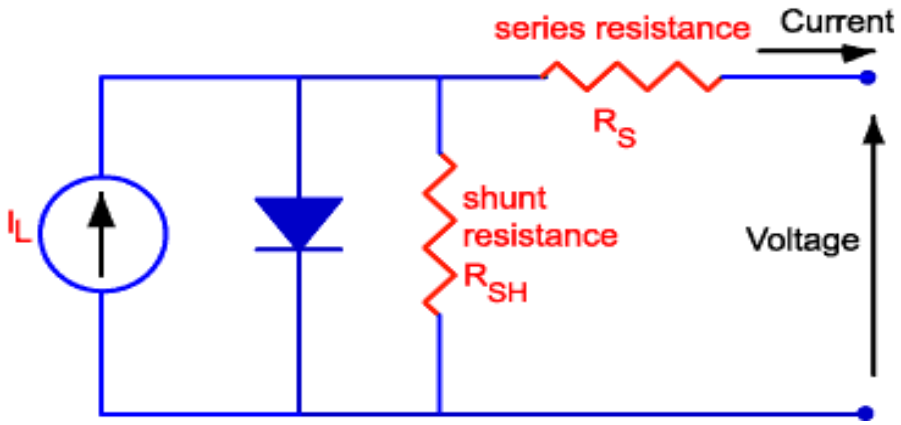

Figure 1.7 Circuit representation of parasitic elements in PV cell

The parasitic elements which a PV cell contains are shunt resistance (R_{SH}) and series resistance (R_{SE}). Due to impurities present near the p-n junction it gives rise to shunt resistance and high resistance of metal contacts, interconnections and semiconductor material give rise to series resistance. The output power of PV cell is increased by the lowering the value of series resistance and in increasing the performance of PV cell higher value of shunt resistance is required.

$$I = I_L - I_O \left[exp\left(\frac{V + IR_S}{\frac{nkT}{q}} \right) - 1 \right] - \frac{V + IR_{SH}}{R_{SH}} \tag{1.6}$$

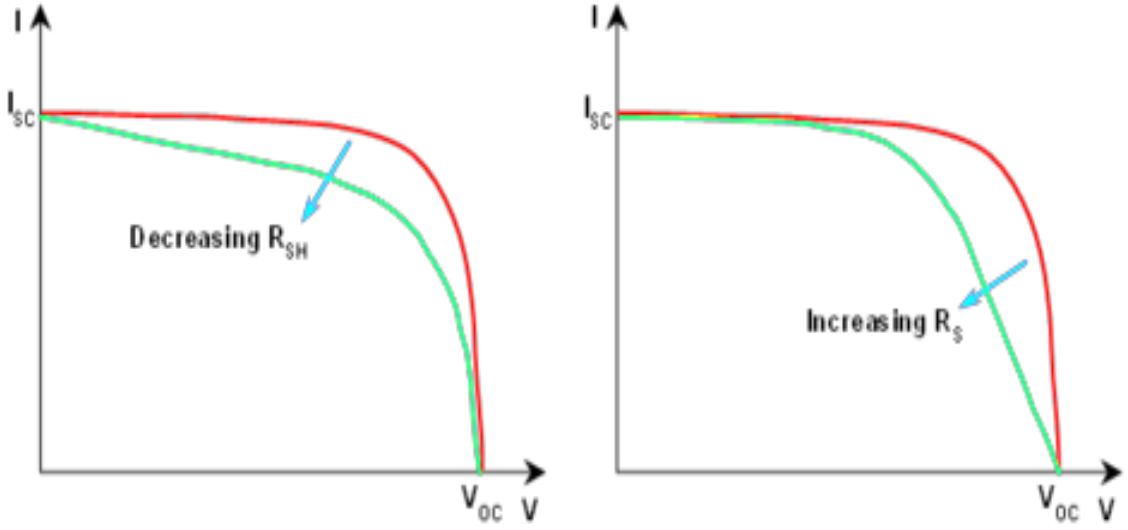

Figure 1.8 On a solar cell V-I curve showing the effect of shunt and series resistance

CHAPTER 2: TWO STAGE POWER CONVERSION FOR GRID CONNECTED PV

Connection with directly to the grid of the PV modules, is not possible hence for the grid connected PV applications there are many current control schemes that have been done. [6]. With their higher efficiency values in the MPPT applications the buck and the boost converters can be used. However, usage in PV supplied systems having the buck converter has limiting usage due to the pulsating the input current [7]. The most commonly used algorithm previously for tracking MPP is perturb and observe (P&O) due to its simplicity in nature, yet around the MPP of the system there are oscillation. Another important issue is inverter current control [7].

Grid conditions such as phase sequence, phase angle and appreciate harmonic levels specified by the grid authorities must condition the inverter current. The method that offers strong robust control, is simple in implementation and provides fast dynamic response is the hysteresis current control method [6] . However, it also has certain limitations i.e. steady-state error and variable switching frequency are two things it suffers in the grid current. In grid connected inverter applications LCL filters are widely used. The LCL filter provides more compact and efficient designs and it is a third order filter [6].

2.1 PV SYSTEM MODELLING

This PV system modelling section consists of PV array modelling, dc-dc boost converter and inverter modelling.

2.1.1 PV ARRAY MODELLING

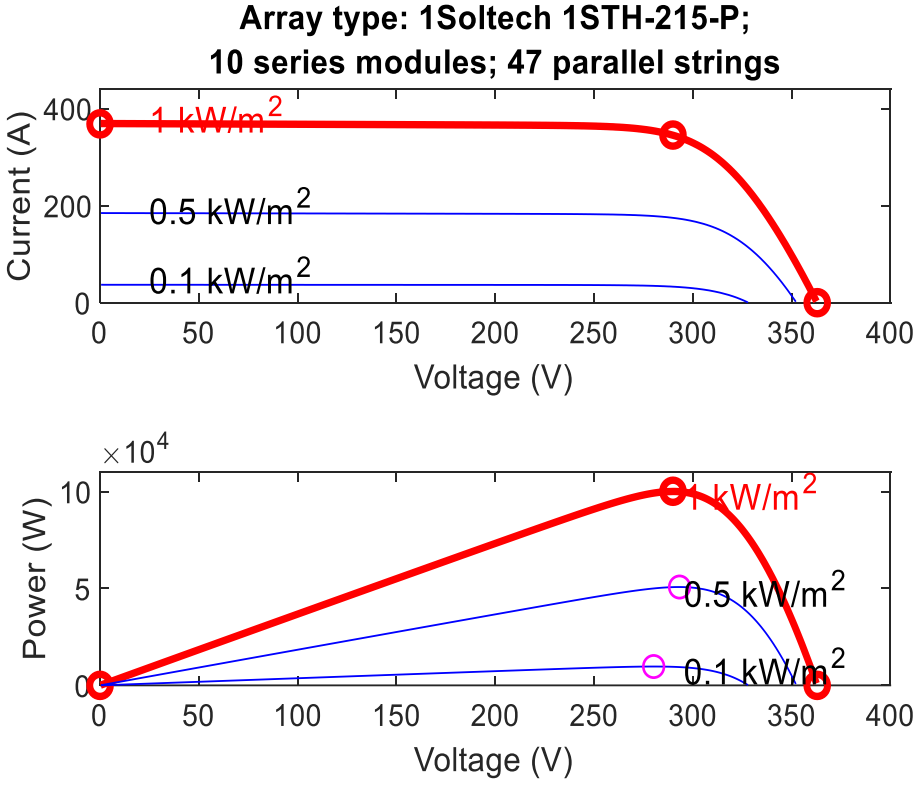

Figure 2.1 PV array characteristics for different solar irradiation values when temperature is constant (a) I-V (b) P-V

The increase in voltage of the module produced is seen when there is increase in no. of series cells and the increase in the current of the module generated is also seen when the no. of parallel modules are increased. In this thesis PV array model simulation is simulated for different irradiation values when temperature is kept fixed with value T = 25˚C and for different temperature values when irradiation is kept fixed with value G = 1000W/m^2, to show the variation effects of irradiation and temperature on the PV array. According to obtained (I-V) and (P-V) characteristics presented in Figure 2.1, PV array current is linked to the strong dependence to the irradiation in which the MPP of the PV array is affected strongly.

Yet it is observed that the increase in the voltage is seen and it is important to note that during the day the temperature variations are generally of no major importance.

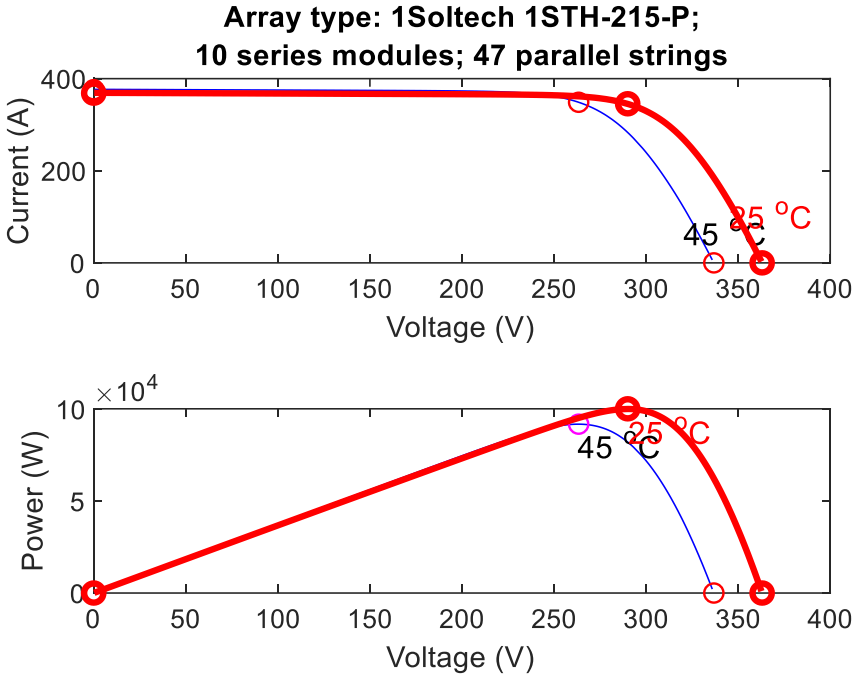

Figure 2.2 PV array characteristics for different temperature values when irradiation is constant (a) I-V (b) P-V

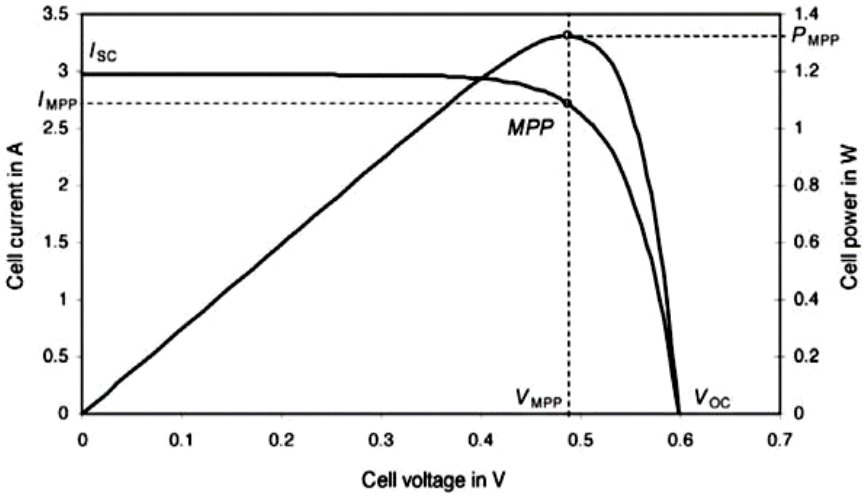

Figure 2.3 P-V and I-V curve with MPP

Therefore, on the I-V curve a dynamic point exists called the maximum power point MPP. So the entire system needs to execute at its maximum power as shown in Figure 2.3.

Table 2.1 Photovoltaic module specifications

Short circuit current denoted by I_{SC}	7.84A
Open circuit voltage denoted by V_{OC}	36.3V
Current at maximum power point denoted by I_{MPP}	7.35A
Voltage at maximum power point denoted by V_{MPP}	29V
Number of cells in series denoted by N_S	60
P_{MAX}	213.15W

2.1.2 DC-DC BOOST CONVERTER

In this system boost type converter with a freewheeling diode is used that helps in amplifying the output voltage of PV array to higher level as well blocks the reverse current. A boost converter is designed using Insulated gate bipolar transistor(IGBT). The signal for switching on/ off the IGBT is generated by DC-DC PWM generator with a switching frequency of 5 kHz. A duty signal is applied to the input of the PWM generator and duty signal is generated by the MPPT algorithm. A bidirectional converter is connected at battery side. The on state resistance of the IGBT (Ron) is set to 0.001Ω and 0.8V is the forward diode voltage drop. The IGBT switching frequency is provided by a pulse generator with switching frequency of 5000Hz. Input resistance (R_{in}) is seen by the PV array source and it can also be determined by the duty cycle. The effective input resistance R_{in} can be determined in (2.1).

$$R_{in} = \frac{R_{load}}{D} \tag{2.1}$$

where R_{load} = resistance of the load
D = duty cycle

Now if ΔI_L is peak to peak ripple current of the inductor of the boost converter, then it can be determined in (2.2)

$$\Delta I_L = \frac{V_{in}.D.(1-D)}{f_{sw}.L} \tag{2.2}$$

where V_{in} = input voltage from the PV array
f_{sw} = switching frequency
L = 5μH

Similarly, if ΔVc is the peak to peak ripple voltage of the capacitor of the boost converter and it can be determined in (2.3)

$$\Delta V_C = \frac{V_{in}.D.(1-D)}{8Lf^2{}_{sw}C} \tag{2.3}$$

where C = 3300μF

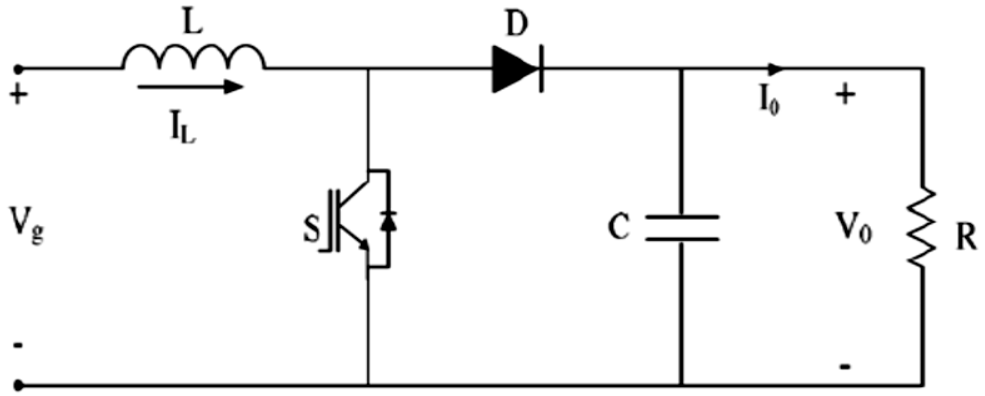

Figure 2.4 Modeling of the boost converter

2.1.3 INVERTER

In the system inverter with IGBT is used that converts the DC supply into AC supply. Current should be molded into the sinusoidal waveform and then with low harmonics content transform the current to ac current. Within the standards, grounding, island detection, etc the inverters should have power quality in grid connected PV system. In PV ystem full-bridge inverter is mostly used. The inverter could be unipolar or bipolar depending on the shape of the output voltage waveform.

2.2 MAXIMUM POWER POINT TRACKING TECHNIQUE

Maximum operating point identification is the major focus while designing a PV generation system. MPPT ensures the highest level of output efficiency but being disturbed by the environmental conditions such as temperature and irradiance. Also in determining the PV system's maximum power operating point the power converter plays the major part. It is observed from the Figure 2.1, 2.2 that the variation of the voltage with the change of irradiation is very small whereas with the increase in temperature voltage is decreased by 2.3mV per ˚C per cell. It can also be seen that each curve has an operating point that can also be observed in these figures for a certain operating voltage and this is the point at which the module produces the maximum power. Then adjustments are tried in that direction till the maximum power no longer increases further. This method has one disadvantage that it can cause power output to oscillate.

However, the main advantage of this method is its ease of implementation. If the batteries are charged fully and PV production jump loads then MPPT is unable to operate the panel at its maximum point because there is no extra load to absorb excess power. Then the operating point of the PV panel is shifted by the MPPT from the peak point until demand is matched. For example in spacecraft to operate the panel continuously at peak power point the extra power is diverted to the resistive load so that it can maintain working on peak point. Voltage or current conversion, regulation and filtering are provided by the integration of electric power converter system and MPPT devices together. So MPPT can be defined as the process of adjusting the load characteristic as the conditions change [8]. Now to overcome the drawbacks of the P&O method, the change in power caused by the irradiation variation is decoupled by the proposed MPPT and also the simultaneous increment perturbation. PI controller of the dc voltage control by making the use of the signal error, estimation of irradiation variation is done. Hence, the irradiation variation, causes the change in power and is reflected by the signal error.

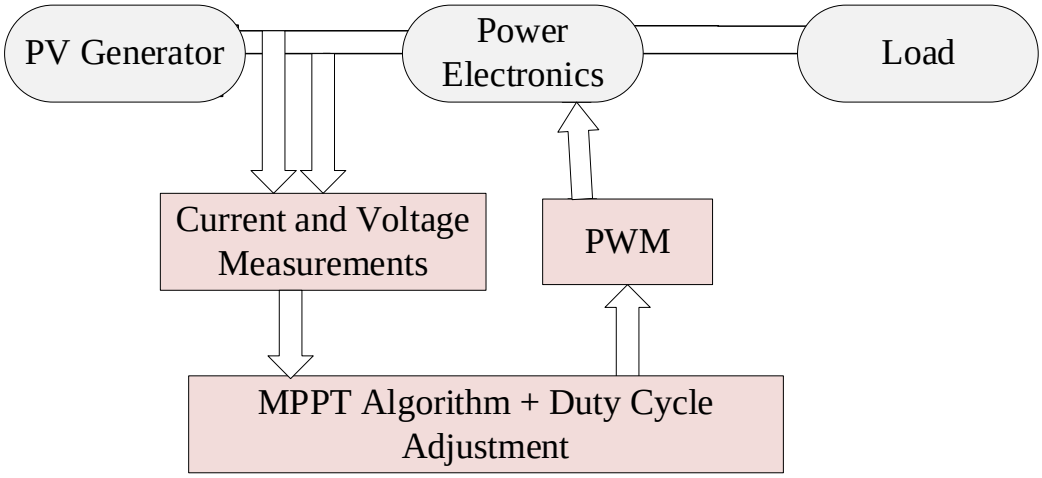

Figure 2.5 The high level schematics of MPPT method

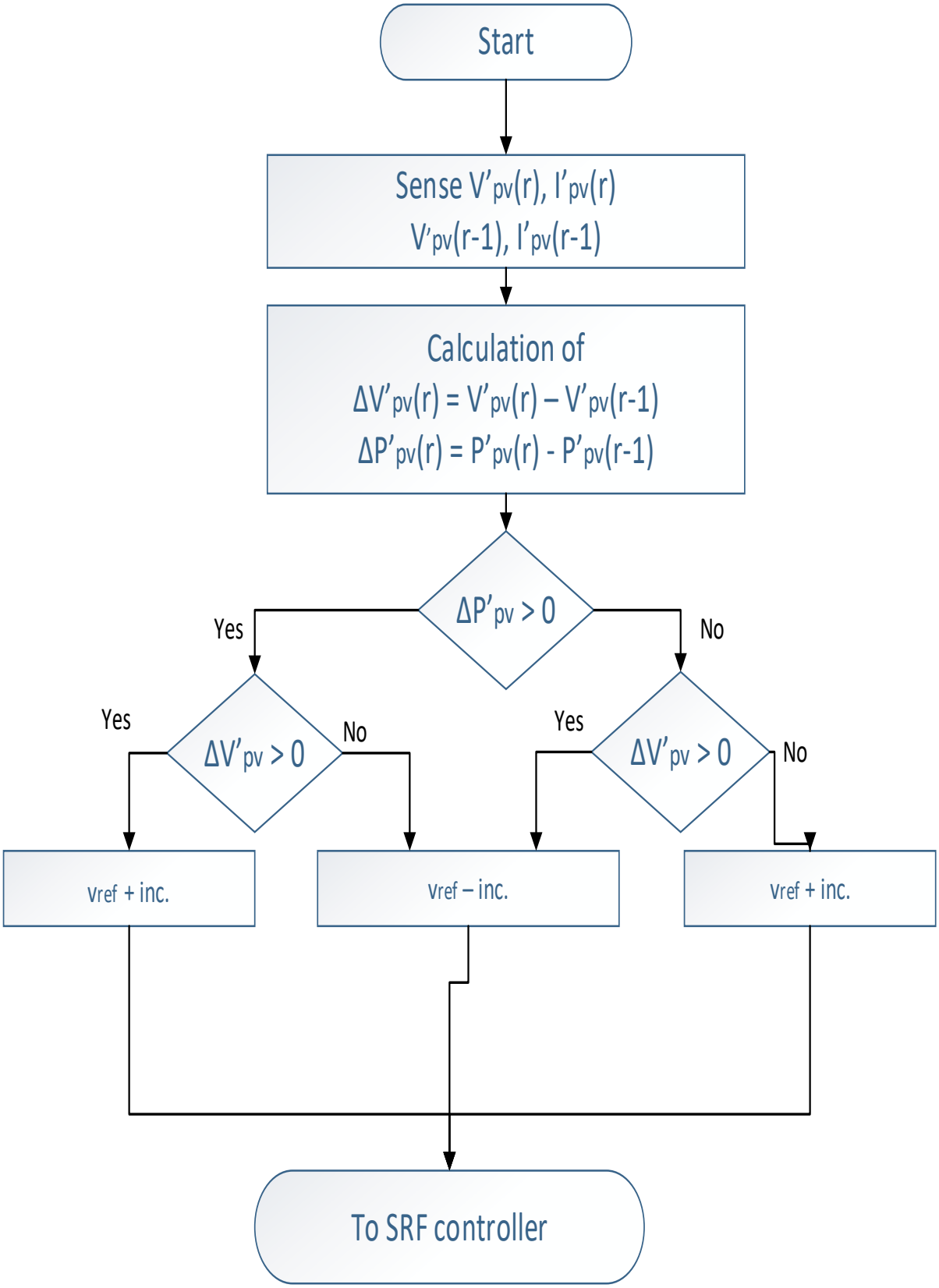

Figure 2.6 Perturb and Observe based MPPT flowchart

2.3 CONTROL SCHEME FOR THE SYSTEM

DC voltage is provided at the input with bus capacitor across it. It is then connected to inverter bridge made using IGBT. The output of the inverter is then connected to an LCL filter. So 3-phase, 3 wire connection is obtained at the output. Now to implement the controller, voltages V_{abc} (L-L voltages) need to be sensed. Then these abc voltages are transformed to 2-phase α-β voltages using Park's transformation. In Figure 2.7 now to sense the inverter current either inverter current or grid current can be used. Here the inverter current is used, then using Park's transformation these currents are transformed to α-β domain and then using Clark's transformation back to d-q domain.

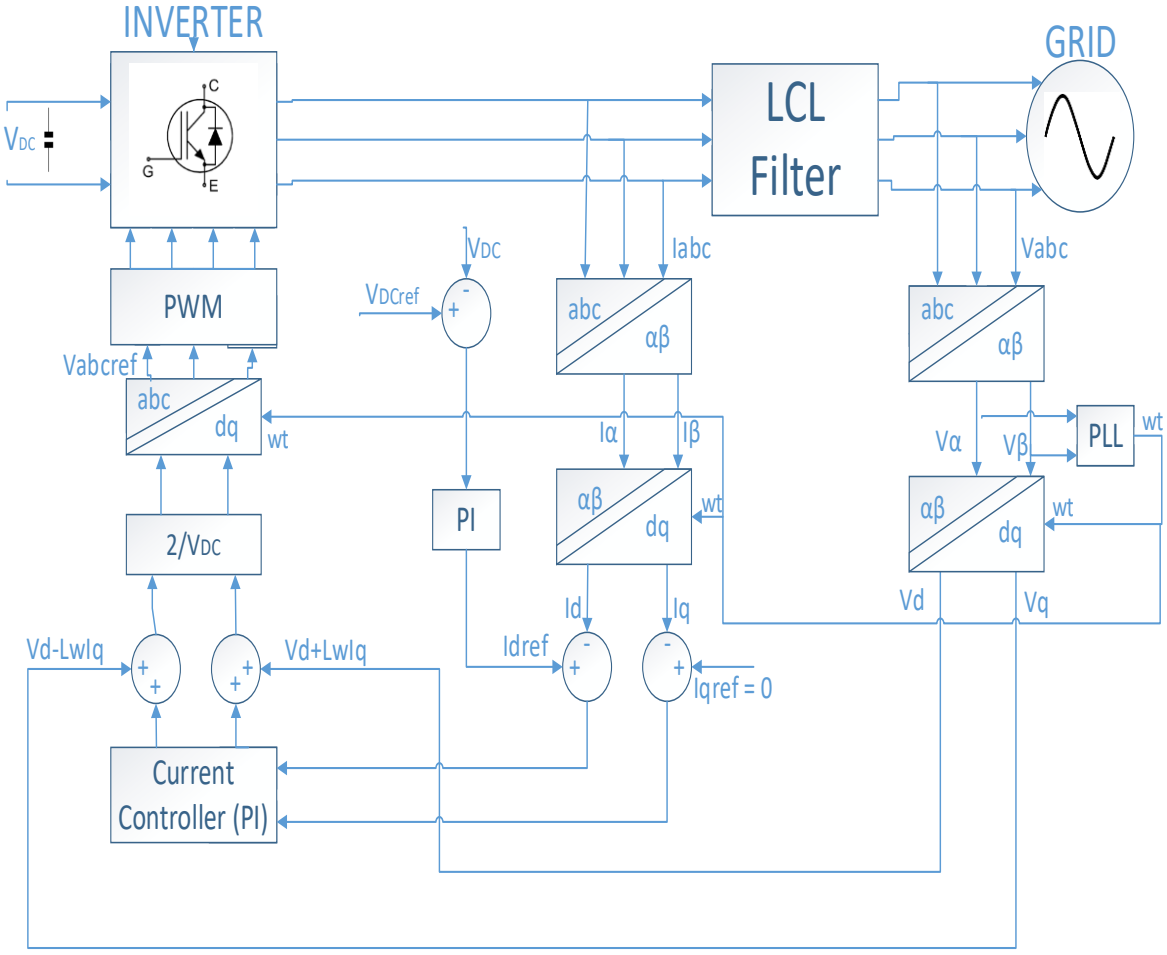

Figure 2.7 Schematic representation for the control scheme of system

Active current is denoted by the I_d and reactive current is denoted by the I_q. Then subtraction of I_d and I_q takes place from reference current to find the error. To find V_d and V_q error is fed to PI controller. For PWM reference current to find the error. Then PI controller is fed with error to find V_d and V_q. Therefore V_d & V_q are multiplied by $2/V_{dc}$ to obtain E_d and E_q. To get the reference for PWM generation it is then transformed to abc voltages and finally PWM generation block is used to obtain pulses.

$$P = \frac{3}{2}\left(V_d . i_d + V_q . i_q\right) \tag{2.4}$$

$$Q = \frac{3}{2}\left(V_d . i_q - V_q . i_d\right) \tag{2.5}$$

However, the average value of V_q is always equal to zero in steady state. So, d-axis current, is the component on which its active power depends and the q-axis current, is the component on which its reactive power depends. Furthermore, fundamental current flow and the eq. becomes

$$P = \frac{3}{2}(V_d . i_d) \tag{2.6}$$

$$Q = \frac{3}{2}(V_d . i_q) \tag{2.7}$$

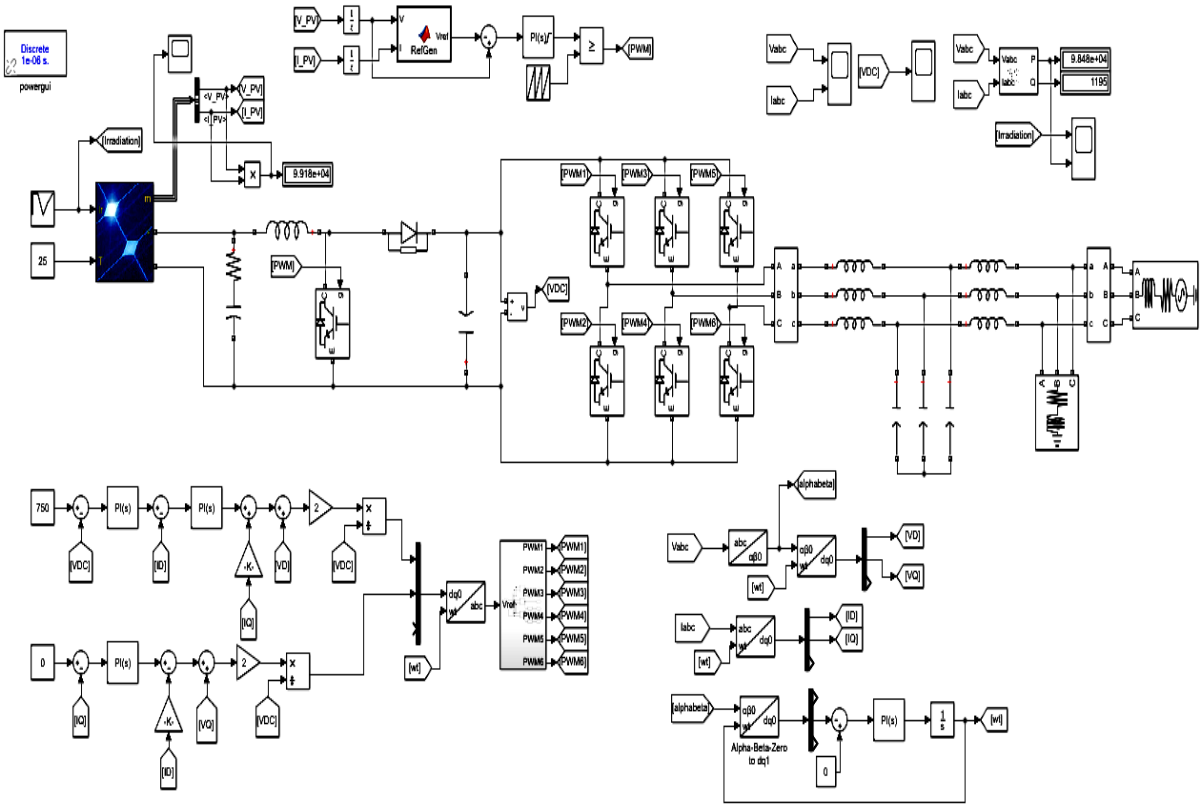

Figure 2.8 Simulink model of the system

For the three-phase inverter the basic techniques are the same. For three-phase PWM inverter, SVPWM control scheme in PV generation system was proposed. SVPWM modulation technique has major advantages. SVPWM modulation technique has some disadvntages also which are variation of the current is sensitive to regulator of current due to time delay, sampling time and non-linearity of the system.

In this model different methods are used to calculate the resistance parallel and resistance series. For example, 1Soltech 1STH-215-P is made of 60 solar cells in series and provides 213W of nominal maximum power. The maximum power point's voltage is 29V and 7.35A is the current delivered at MPP. In the PV array there are 47 parallel strings connected and each string contains 10 series-connected modules. The parameters of the 1Soltech 1STH-215-P are given in table 2.1 which is essential to model the PV array.

2.4 SIMULATION RESULTS

Table 2.2 System specification

V_{ip}	250V
V_{op}	750V
P	100kW
f_{sw}	5kHz
I_{ip}	100kW/250V=400A
ΔI	5% of 400=20A
ΔV	1% of 600=6V
I_{op}	100kW/600V=166A
V_{oc}	363V
V_{mppt}	270-300V
V_{L-L}	400V rms
L_{filter}	500μH
C_{filter}	100μF
L_{boost}	1.45mH
C_{boost}	3227μF
Ts	1μs

PV array analysis together with the boost converter and resistive load is presented in this simulation shown in this chapter. The irradiance and temperature are varied to determine the performance of the MPPT and track the maximum power of the PV. By adding a three-phase full bridge inverter from the Simulink block toolbox the simulation of the three-phase PV system is realized. Now to generate the PWM signal of the inverter pulse generator block is used. Figure 2.9 shows the settings of the pulse generator With the pulse generator block the carrier frequency, sampling time and modulation index can be set up.

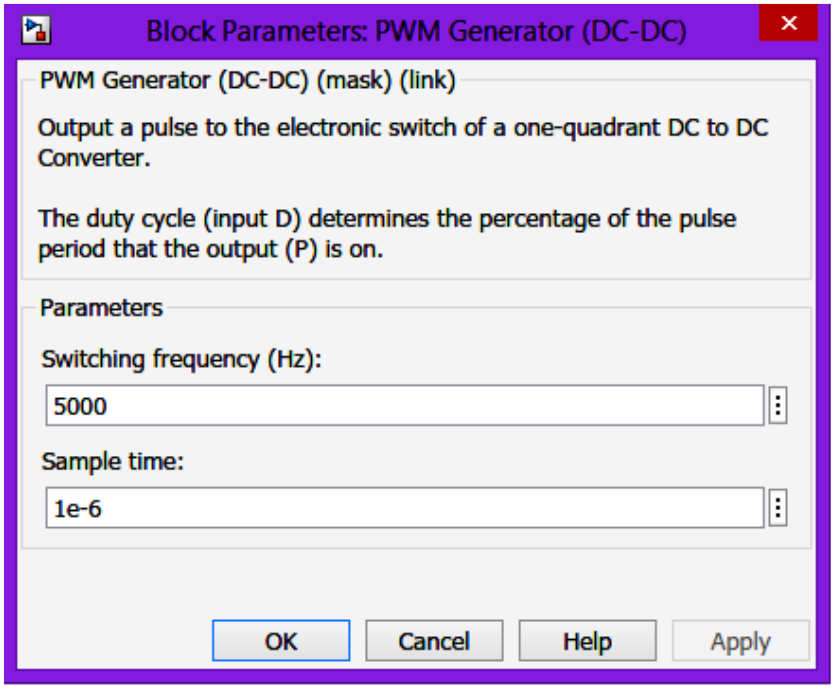

Figure 2.9 Pulse generator

In this chapter we performed two simulations to test the performance of the PV array and the maximum power point controller. When irradiation is changed from 1000 W/m^2 at t = 0.25s to 500 W/m^2 at t = 0.5s the active power also reduces from 100kW to 50kW and then again increased to 100kW gradually at t=0.75s and t=1s, it can be seen in Figure 2.11. Vdc reference link voltage was selected as 750V for the system. Here, we get the Vdc link voltage which settles near about 750V in Figure 2.12.

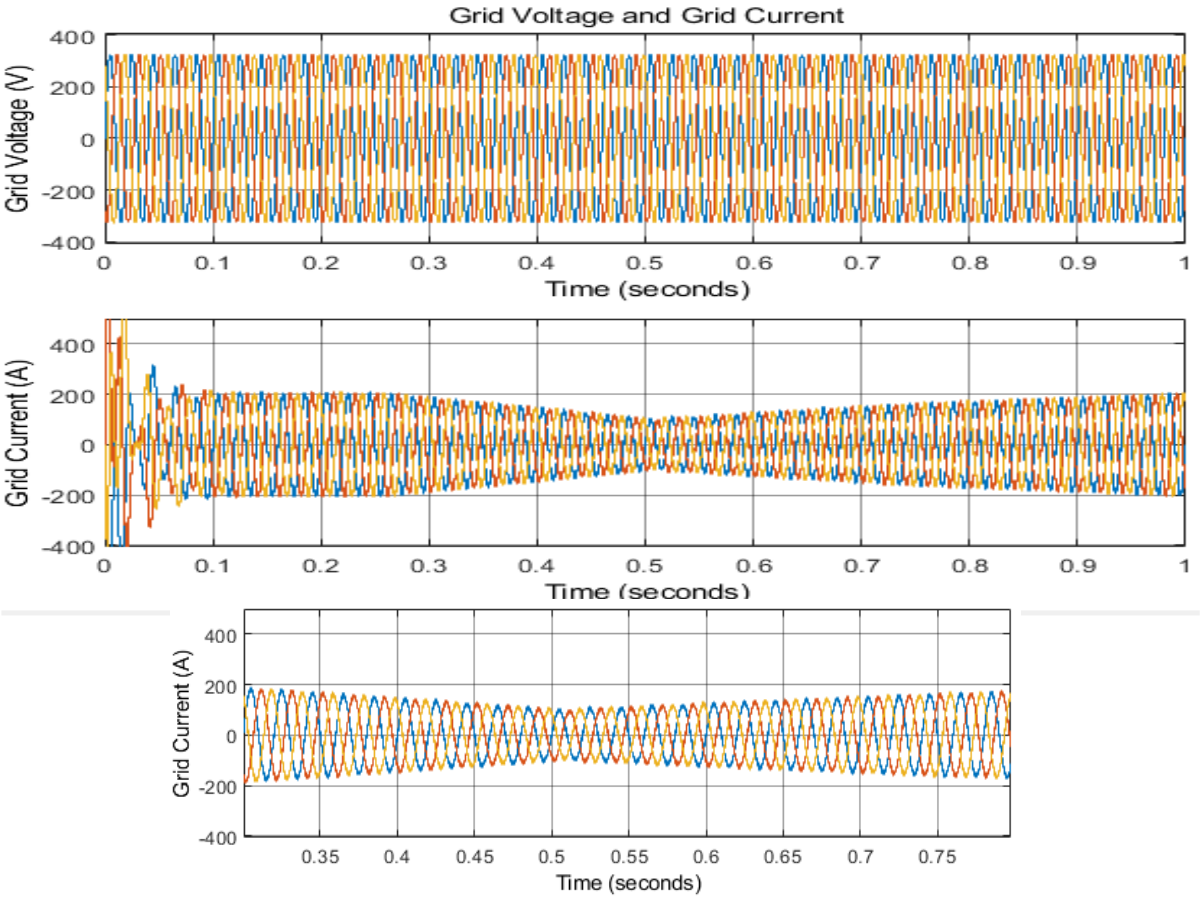

Figure 2.10 Voltage and current of the grid

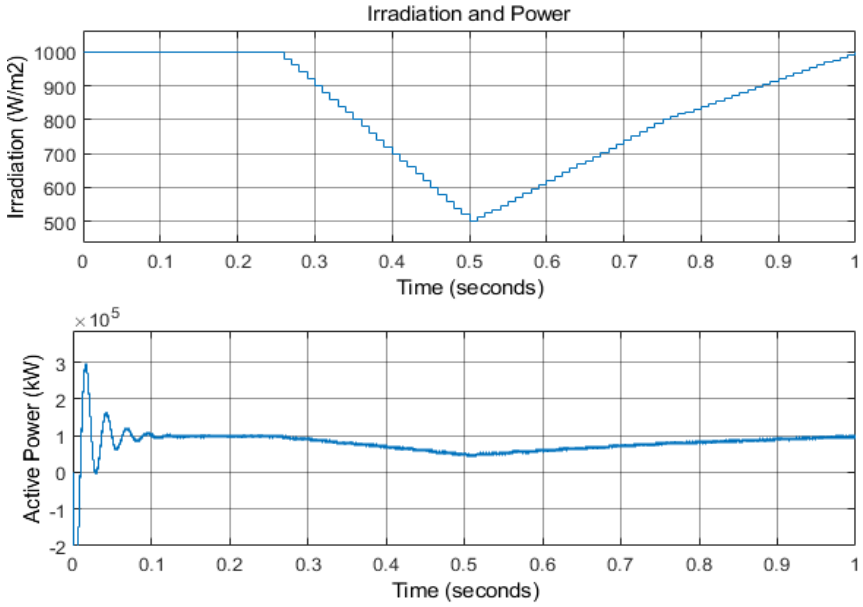

Figure 2.11 Variation of the irradiation and the output power

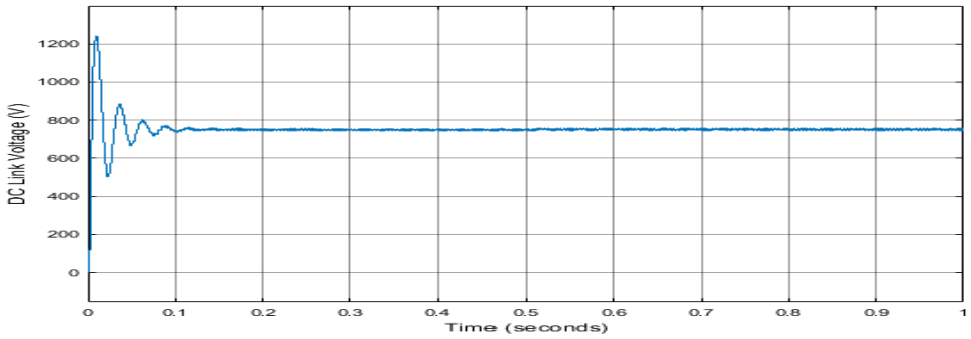

Figure 2.12 DC link voltage plot

In next simulation, initially irradiation is 1000 W/m^2 at t=0s and then irradiation is changed from 950 W/m^2 at t = 0.25s to 550 W/m^2 at t = 0.5s and then again to 1000 W/m^2 at t = 1s the active power also reduces from 95kW to 55kW and then again increased to 100kW at t=1s can be seen in Figure 2.14. Vdc reference link voltage remains same as 750V for the system in case 2 as in case 1 that can be seen in Figure 2.15. From Figure 2.10 and Figure 2.13 it is clear that grid voltage obtained is 363V which is also the open circuit voltage of the PV module. MPPT changes as per irradiation as seen in Figure 2.11 and Figure 2.14.

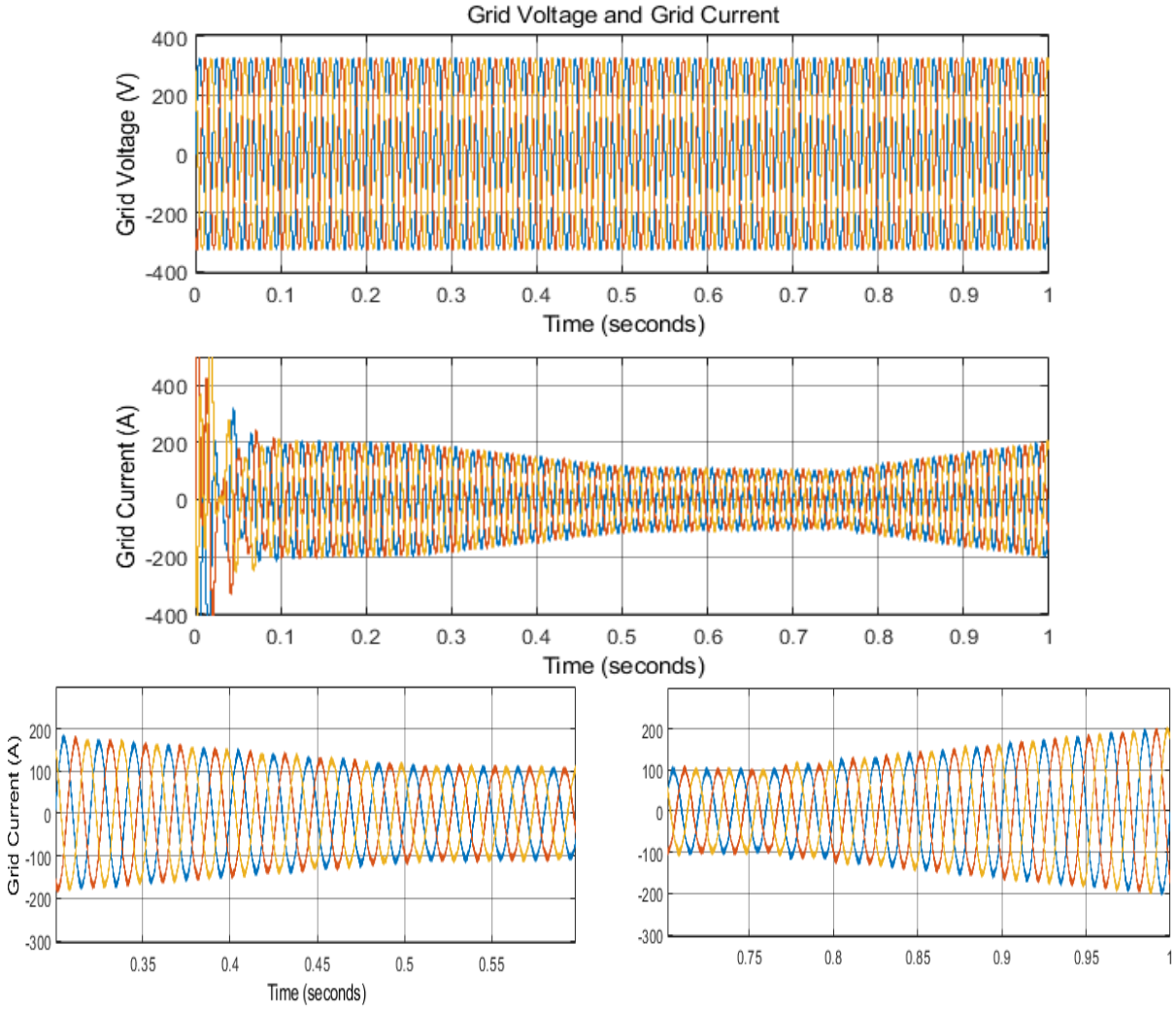

Figure 2.13 Voltage and current of the grid in case 2

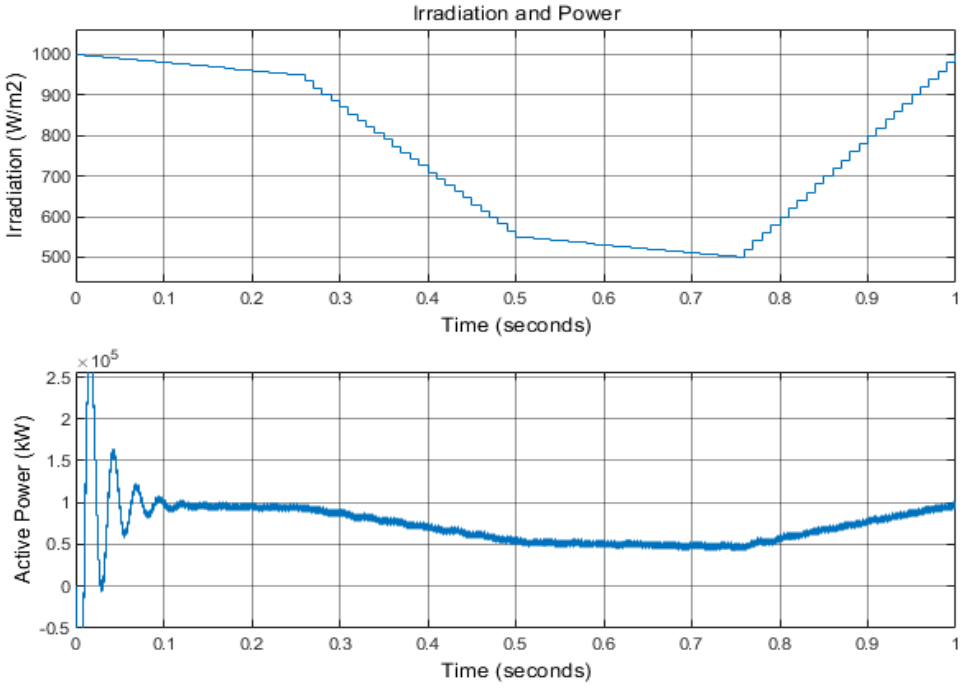

Figure 2.14 Variation of the irradiation and output power in case 2

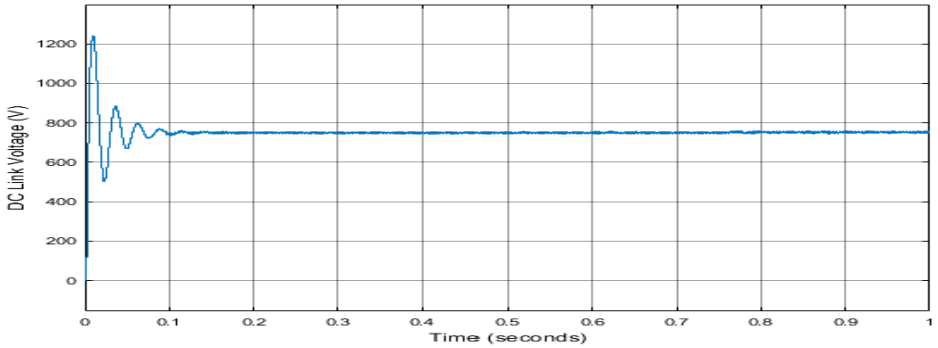

Figure 2.15 DC link voltage plot

2.5 CONCLUSIONS

For a two-stage grid-tied PV system in chapter 2 a high performance control scheme is proposed in paper. SRF theory is the control structure and to maximize the solar energy extraction of each PV string individual MPPT control is realized and to improve the efficiency of the PV system. Hence, it can be concluded that output power depends on the irradiation, moreover for proper inverter operation DC link voltage should remain constant. So, the performance improvement, effectiveness and feasibility of the proposed control scheme from the simulation results obtained are confirmed.

Steady state result are given by the decoupled current control. Results obtained shows that with very low distortion level the grid currents injected to the grid are sinusoidal and after all that a very fast response and good accuracy was offered by the proposed system for all the operating conditions.

CHAPTER 3: PERFORMANCE ANALYSIS OF INTEGRATED PV BATTERY STANDALONE SYSTEM

In this chapter integration of the photovoltaic (PV) array and battery for power generation is discussed. The chapter focuses on design and control of the standalone system in the absence of utility grid. A MATLAB SIMULINK based model is developed such that if there is less generated PV power than the required power for load, then the battery side should feed to the load. The contributions of the chapter include design and sizing of a standalone system comprising PV panel and battery storage system and testing its performance for different situations. The pole mounted arrays have a major advantage over others as for more cooling they are open and have air on their underside which also increases their performance. [1-2]. Two main issues are considered for the improvement of the performance of the tracking system. First, the sunlight is perpendicular to the solar panel and thus more sunlight is received as compared to the case if it were at any other angle. The second is that direct light is used more efficiently than angled light. A PV-battery system is considered and designed in this chapter. Since, the PV power is not available at all times, the control is designed by integrating battery also. Whenever the demand of load is more or will not be fully met by the primary solar energy source, it will be supplied by the battery. Moreover, when the load demand will become less than the generation, the PV source will charge the battery as well as supply to the load. However, the utility grid is not considered in this chapter. The goal of this work is to model and analyze a PV system integrated with battery storage systems using bidirectional DC-DC boost converter. There has been increased use of batteries in PV system so that energy can be stored and used at night. The most popular batteries used nowadays nickel cadmium, lithium ion batteries and lead acid batteries. Some other types of batteries used for PV system are sodium sulfur and vanadium redox. Integrated battery with PV system need a charge controller and more advanced controllers logic into charge their battery charging algorithms by using use maximum power point tracking (MPPT) [2].

3.1 PV ARRAY AND MODULE

Less than 3W of power at 0.5V DC is generated by the PV cell hence it is not used practically. Hence to generate suitable power multiple PV cells in parallel-series combination are used. To achieve the suitable output voltage 36 or 72 may be connected in series. For a 36 PV cells connected in series a typical layout is presented in this Figure 3.1. In this chapter model is of 1kW, PV module consist of 5 parallel strings in which series-connected modules per string is 1 and thus a total of 213.15W of power is generated by the PV panel. When cell becomes partially or entirely shades the overall performance of the module is thus degraded that means the PV cells are connected in series. To act as a load instead of generator the shaded cell can be reverse biased. Now to avoid the impact of shaded cell on whole module the bypass diodes are connected in an anti-parallel combination as shown in Figure 3.2. of the system, PV modules are connected in parallel. A series-parallel combination of PV modules is shown in Figure 3.3.

To increase the voltage capacity of PV array, PV modules are connected in series and to increase the current capacity.

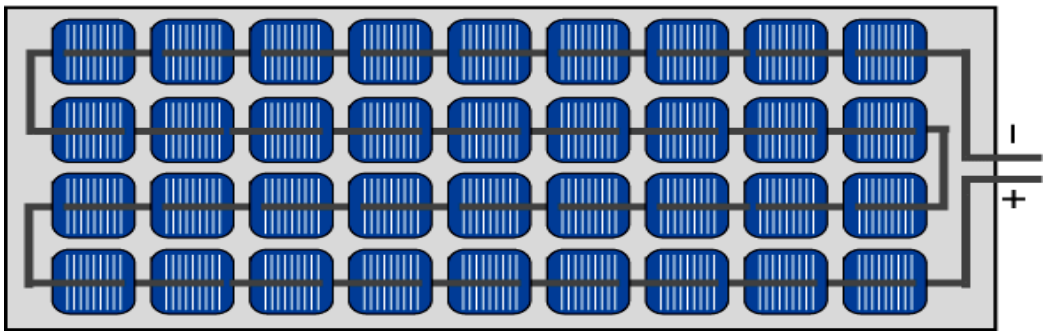

Figure 3.1 36 cells PV module structure connected in series

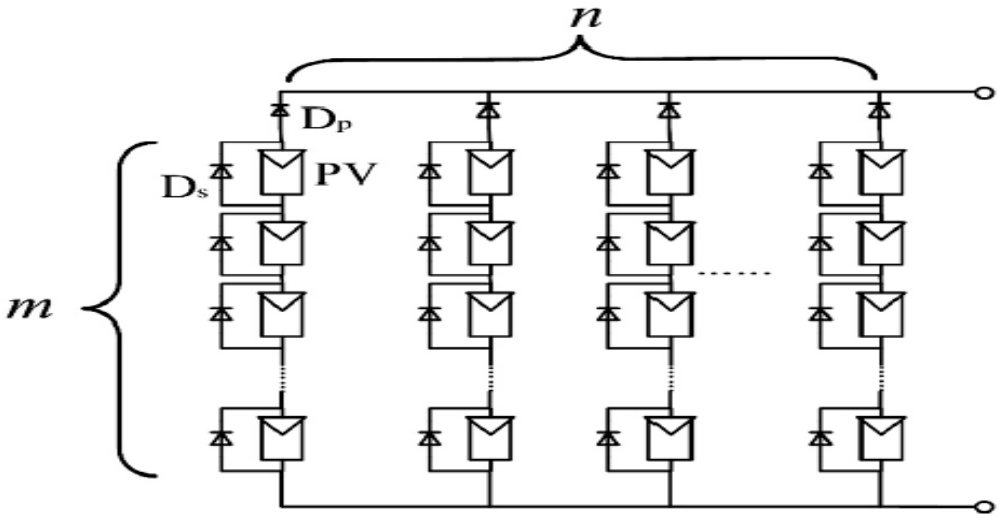

Figure 3.2 PV module cells with bypass diode

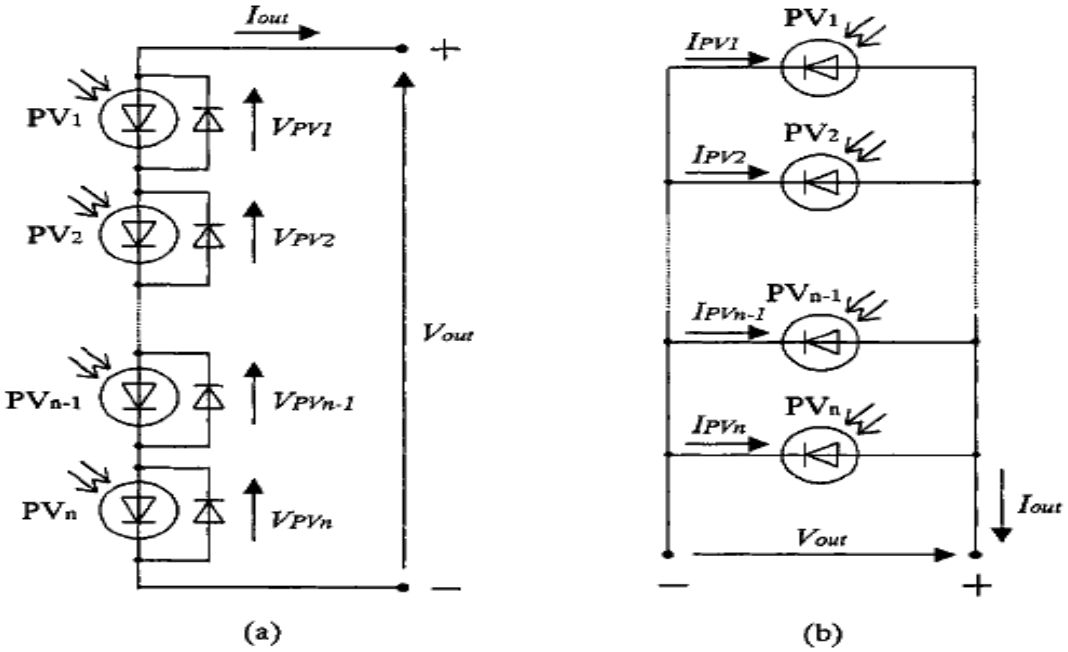

Figure 3.3 PV modules (a) in series (b) in parallel

3.2 BATTERY STORAGE [18]

By using the electrochemical reactions energy is stored and released by the batteries and battery is said to be in charging mode when electrical energy is converted into chemical energy.

3.2.1 COMPONENTS OF BATTERIES AND CELLS [18]

1. CATHODE : It is oxidized by supplying electron to the external circuit and is oxidizing by absorbing electron from the external circuit.

2. ANODE : It is accepting electrons i.e, it is oxidizing from the external circuit and by supplying electron through the external circuit it gets oxidized.

3.ELECTROLYTE : It is a material which can be either acidic solution or alkaline solution and thus conducts electric current as sepration into positively and negatively charged particles called ions.

3.2.2 CELL'S OPERATION CHARGING AND DISCHARGING [18]

To the load when the battery cells are connected movement of the electrons start from anode to cathode.

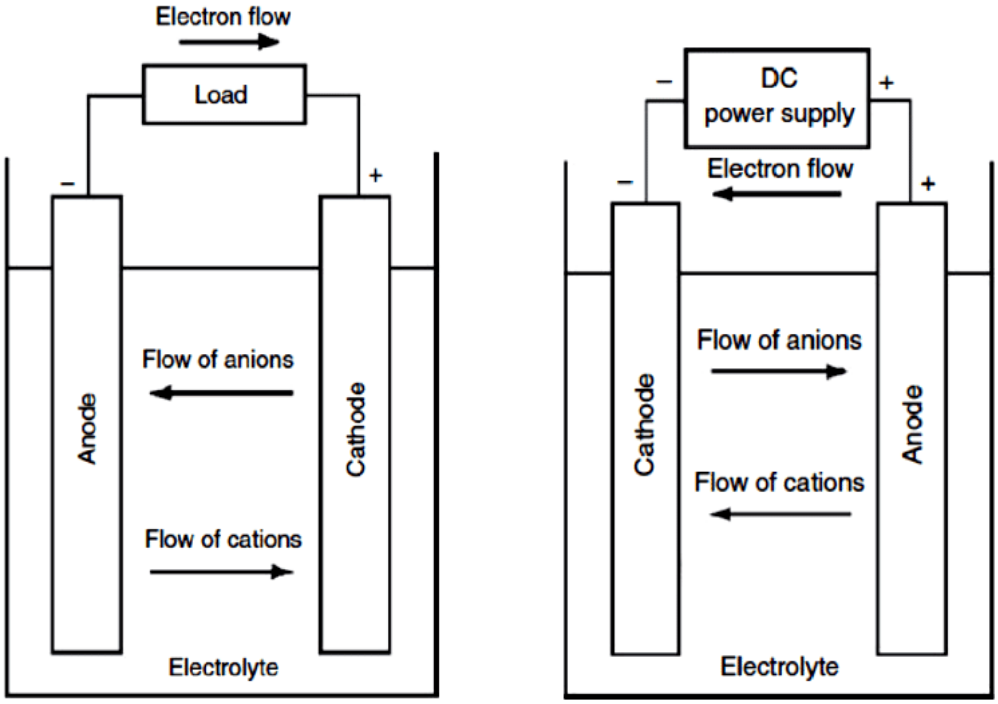

Figure 3.4 Discharging and charging of a cell

The current flow is reversed during the recharging of a battery cell. The operation of discharging and charging of a cell is shown in Figure 3.4.

Cathodic reaction i.e, gain of electrons

$$Zn \rightarrow Zn^{2+} + 2e^{-} \tag{3.1}$$

Anodic reaction i.e, loss of electrons

$$Cl_2 + 2e^{-} \rightarrow 2Cl^{-} \tag{3.2}$$

Overall reaction

$$Zn + Cl_2 \rightarrow Zn^{2+} + 2Cl^{-}(ZnCl_2) \tag{3.3}$$

3.2.3 CLASSIFICATION OF BATTERIES [18-19]

1. PRIMARY BATTERIES : These batteries can only be used once and are irreversible batteries because of its chemical reaction. These batteries are cheap and easy to use so they are common for small usage.

2. SECONDARY BATTERIES : Secondary batteries can be used again and again because of their discharging/charging capability and thus are called reversible batteries. These batteries are highly used in automotive and industries application because of their capability to deliver high currents and their rechargeable characteristics. Examples of these batteries are lithium ion, nickle/cadmium and lead-acid type batteries.

3.2.4 LITHIUM-ION BATTERIES

Using graphite carbon the positive electrode of Li-ion batteries is made and using the lithium metal oxide ($LiXO_2$) the negative electrode is made. The V_{OC} of the cell is 4V. The major differentiate characteristic of the Li-ion battery comparing to other conventional batteries is that it has higher energy storage.

3.2.5 LEAD-ACID BATTERIES

Using lead(Pb), negative electrode of each cell of lead-acid battery is made whereas using lead dioxide(PbO_2) positive electrode is made. Sulphuric acid is taken as electrolyte and it consists of a separator that keeps electrodes electrically apart. Lead-acid batteries are used as UPS (uninterruptible power supply) and car starters as they are low-cost batteries.

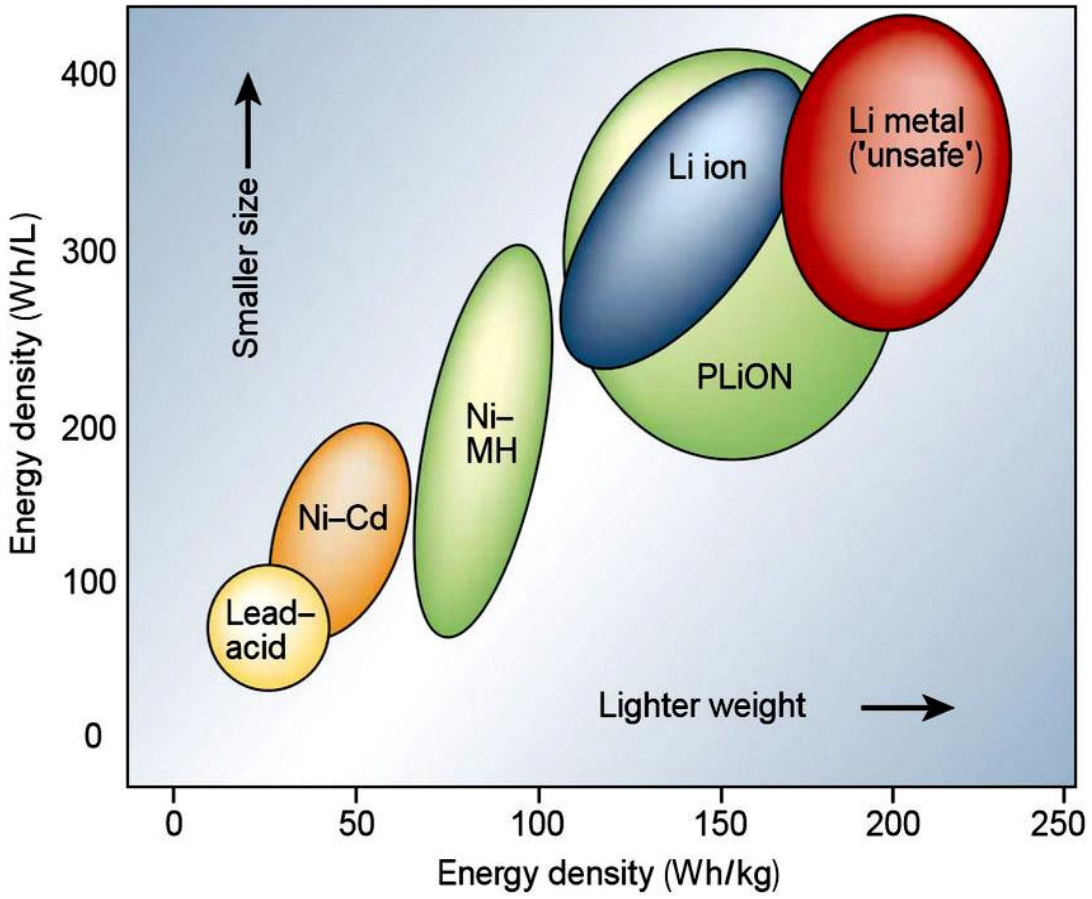

Figure 3.5 Energy density (Wh/l) and specific energy (Wh/kg) for the small rechargeable batteries [19].

3.2.6 SIZING CALCULATION

Stand-alone PV system sizing is based on four fundamental calculations [20]. First is the energy demand requirements on the load side is decided by the load analysis. Second is to determine the critical design month, the availability city data insolation is compared with monthly load requirements. Third is, PV arrays reduce outputs during cloudy days. Last is the PV arrays should be sized such that for both load requirements and battery they can generate enough power.

3.2.7 BATTERY SIZING

PV array which generate excess of energy during sunny and high insolation of periods, then these energies are stored by these batteries. When there is no solar energy, then time during which from the beginning a lonely battery provides power for load requirements from a full state of charge then it is defined as autonomy day. With larger and higher cost battery banks greater autonomy days are associated. The battery capacity is calculated by the following equation;

$$B_{out} = E_D . \frac{t_a}{V_{SDC}} \tag{3.4}$$

$$B_{rated} = \frac{B_{out}}{DOD_a . V_{SDC}} \tag{3.5}$$

where

B_{OUT} = required battery output (Ah)

E_D = daily energy demand (Wh/day)

t_a = autonomy days

V_{SDC} = nominal dc system voltage (V)

DOD_a = allowable depth of the discharge

3.3 PARAMETERS OF BATTERIES [19]

1. STATE OF CHARGE (SOC): Battery's relative capacity as the percentage of the battery's maximum capacity is termed as SOC. The fully charged battery represents 100%. Battery aging means the capacity of the battery is deteriorating over period of time. Current drawn/supplied is the common method to determine the status of SOC and the variation in the battery over a certain period of time.

2. DEPTH OF DISCHARGE (DOD): How deeply the battery is discharged is termed as depth of discharge (DOD). State of charge (SOC)'s opposite is depth of discharge (DOD). If the battery DOD is 0% that is battery is fully charged then SOC will be 100%.

3. SELF-DISCHARGE: When there is no load connected or during open circuit conditions the gradual discharge in the available capacity over time is called self-discharge. Various factors such as temperature, electrode material, aging and manufactures affects self-discharge.

4. VOLTAGE: On of the most important parameter considered is voltage, i.e. to provide the electric energy when the batteries charges/discharges. The voltage of the battery is dependent on the power delivered to load and can be observed in the equation. Current density determines voltage i.e. voltage is reduced when more current is drawn from the battery, the voltage and the charge capacity of the battery as shown in Figure 3.6.

$$P = \frac{E^2}{R} \tag{3.6}$$

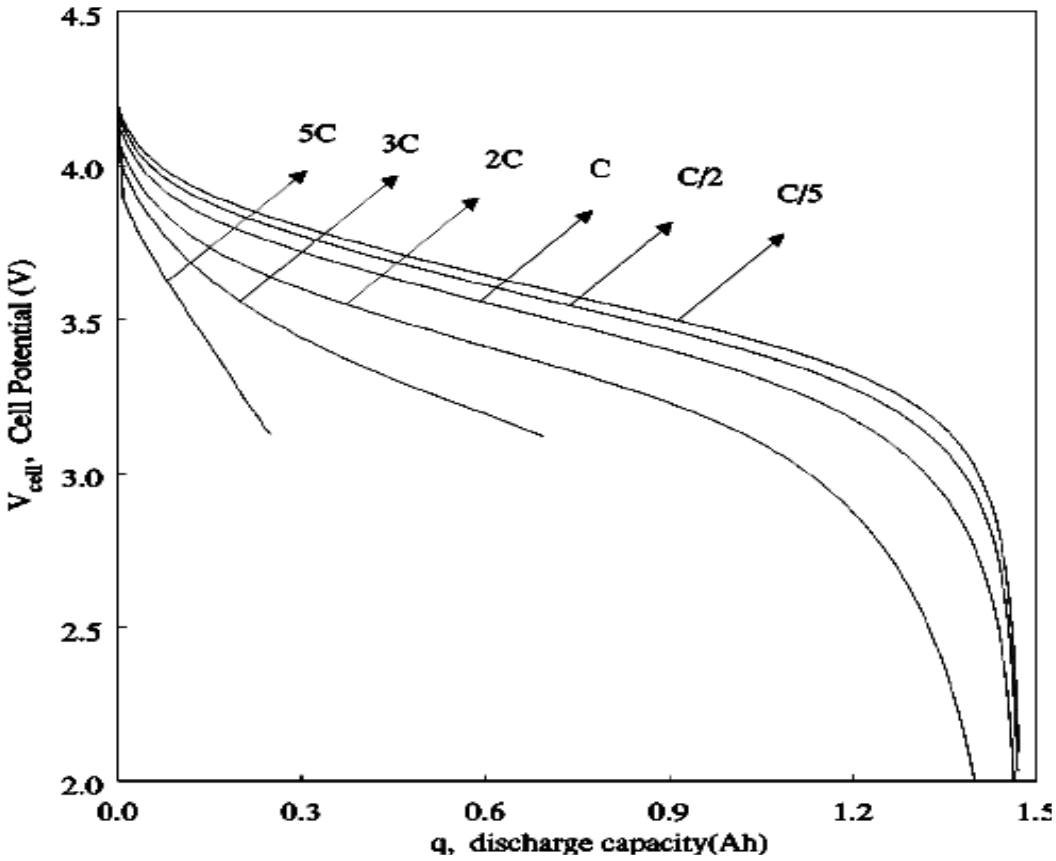

Figure 3.6 Effect of discharge current density on the discharge capacity of the battery

3.4 MAXIMUM POWER POINT TRACKING (MPPT)

The non-linear electrical behavior of the cell is characterized by the fill factor and it is defined as the ratio of the maximum power from the cell to the product of open circuit voltage and short-circuit current.

$$P = FF * Voc * Isc \quad (3.7)$$

where FF = fill factor
V_{OC} = referred to open circuit voltage
I_{SC} = referred to short circuit current

In the Perturb and Observe method [19], voltage from the array is adjusted by a small amount by the controller and then power is measured. Then adjustments are tried in that direction till the maximum power no longer increases further. This method has one disadvantage that it can cause power output to oscillate. However, ease of implementation is the main advantage of this method. If the batteries are charged fully and PV production jump loads then MPPT is unable to operate the panel at its maximum point because there is no extra load to absorb excess power. Then the operating point of the PV panel is shifted by the MPPT from the peak point until demand is matched. Voltage or current conversion, regulation and filtering are provided by the integration of electric power converter system and MPPT devices together. So MPPT can be defined as the process of adjusting the load characteristic as the conditions change. Flowchart for the Perturb & Observe (P&O) based MPPT is shown in Figure 3.7.

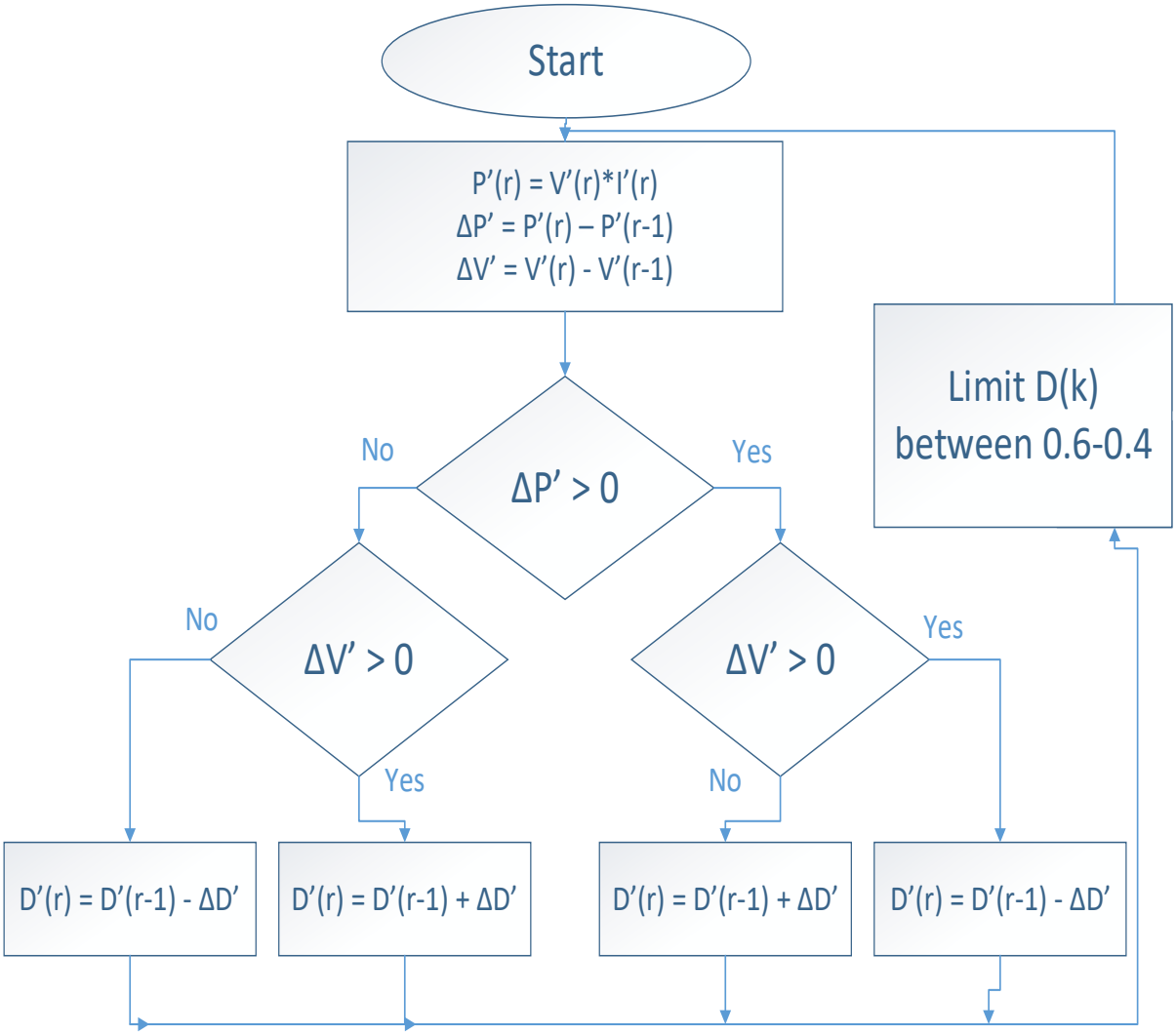

Figure 3.7 Flowchart for the Perturb & Observe based MPPT

3.5 BATTERY CONTROL

Table 3.1 Battery Specifications

Parameters	Specifications
Type of Battery	Lithium-Ion
Nominal Voltage	24V
Initially SOC	45%
Ampere Hour Rating	50Ah
Fully Charged Voltage	27.93V

The level of charge of an electric battery relative to its capacity is known as State of charge (SoC). SoC has been selected as 45% in developed model. Practically SoC is not kept beyond 50% which that means cell starts recharging when the SoC reaches 50%. From Figure 3.8 we can say that if 100% is the charge i.e, maximum level in the battery then the floating state is maintained by the battery [24]. Now if the battery charge is less than the value, then the battery will be charged either at constant current or voltage mode by the control system. The same flowchart for battery controller is shown in Figure 3.8.

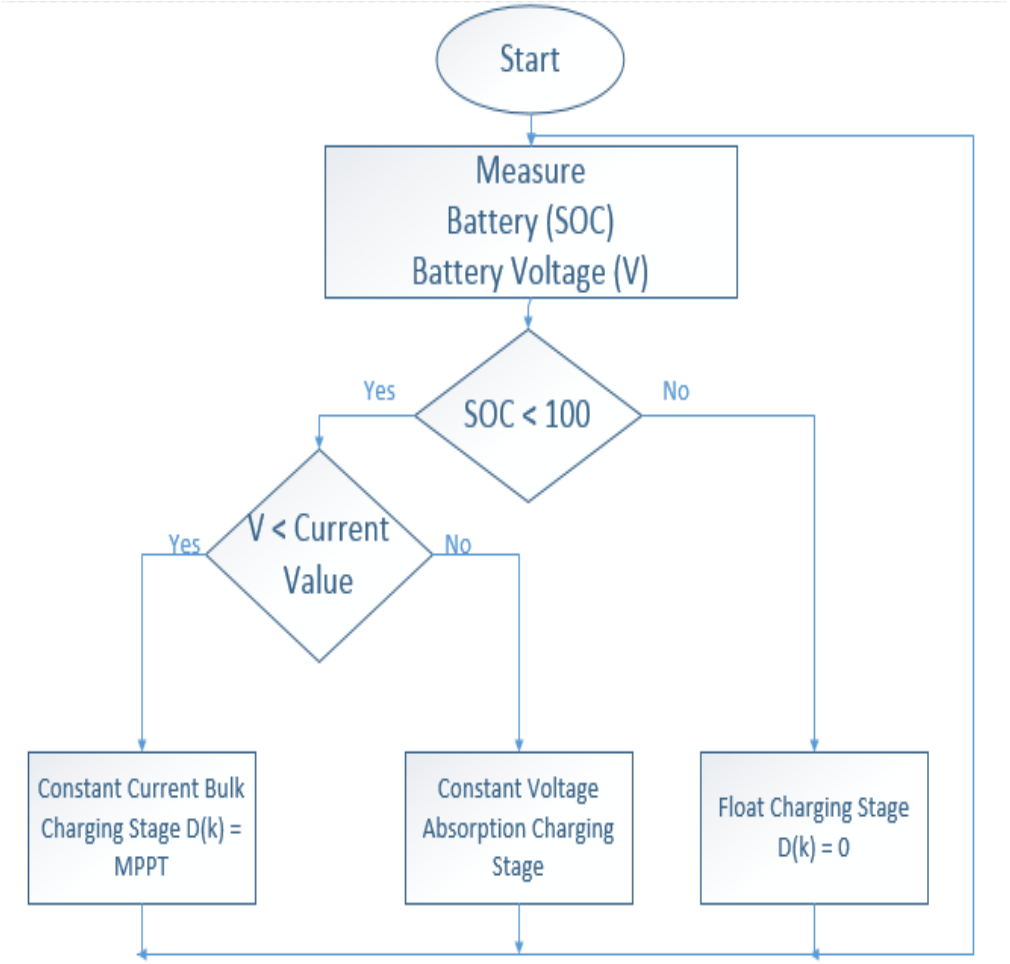

Figure 3.8 Flowchart for battery controller

3.6 METHODOLOGY AND SIMULINK MODEL

The layout of the integrated PV-battery system is shown in Figure 3.9. A common resistive load is used here. Load voltage is kept constant and current is being controlled. Load is connected at the common coupling point. PV side needs maximum power point (MPP) control for tracking maximum power. In another case when PV generates more power than required by the load, then the battery starts charging to maintain the coupling voltage constant. The coupling point of PV and battery requires a large value of capacitor. The representation of the solar photovoltaic battery system with MPPT controller is modelled in MATLAB and shown in Figure 3.10. The model shown here basically integrates load, a 24V battery and 1kW PV source. The details of the battery are already discussed earlier.

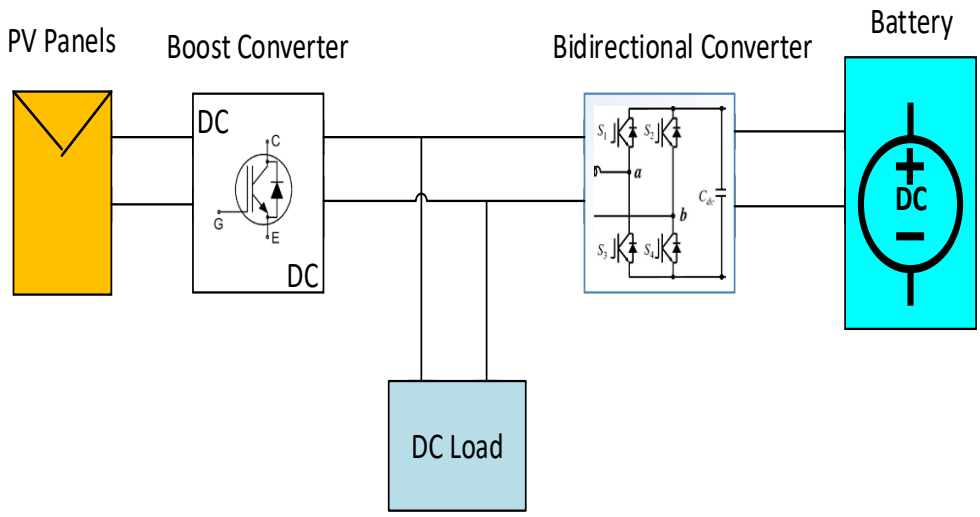

Figure 3.9 Block diagram for the system

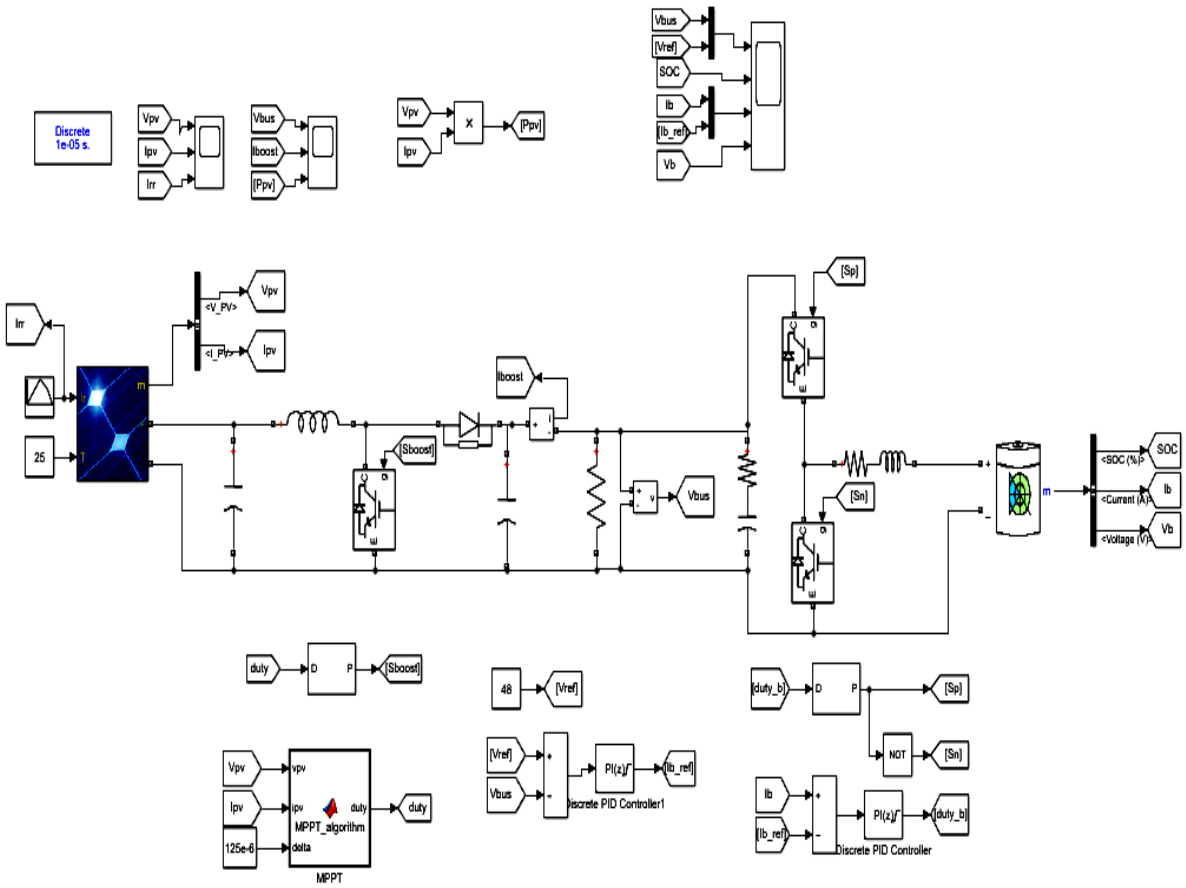

Figure 3.10 Model showing overview of the photovoltaic system with battery controller

3.7 SIMULATION RESULTS

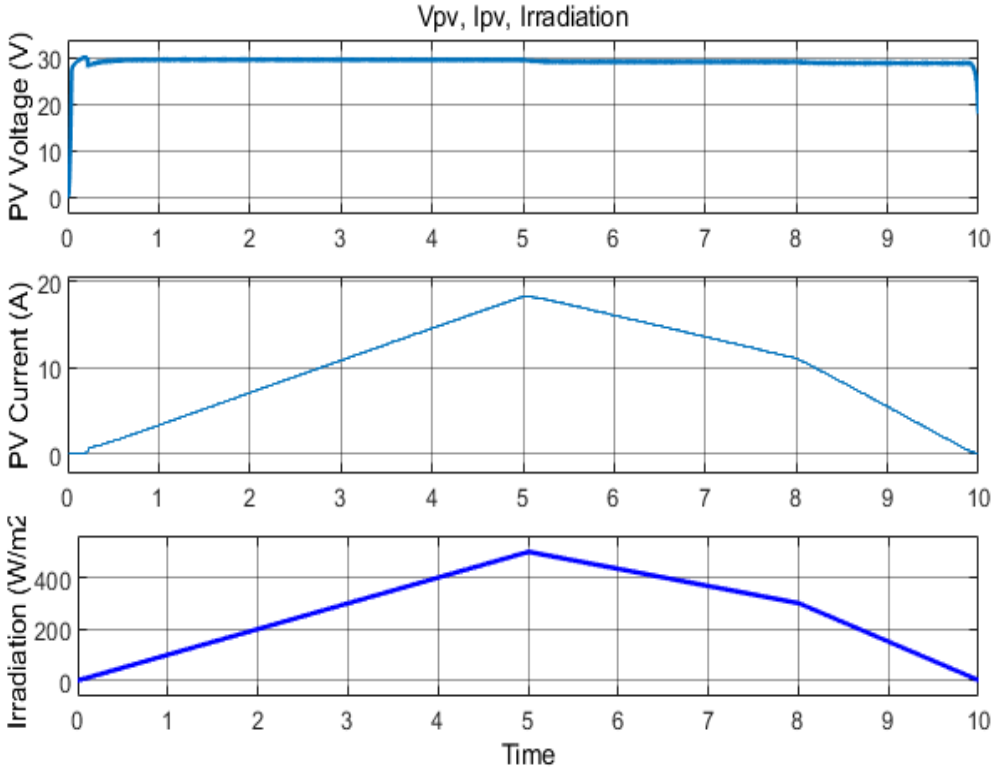

Figure 3.11 Performance Results for MPPT voltage, current and Irradiation change

The solar irradiance is varied from 0W/m^2 at t=0s to 1000W/m^2 at t=10s as shown in Figure 3.11. It is observed that the PV voltage V_{pv} remains constant nearly to about 29V whereas PV current i_{pv} varies as per trend of irradiation variation.

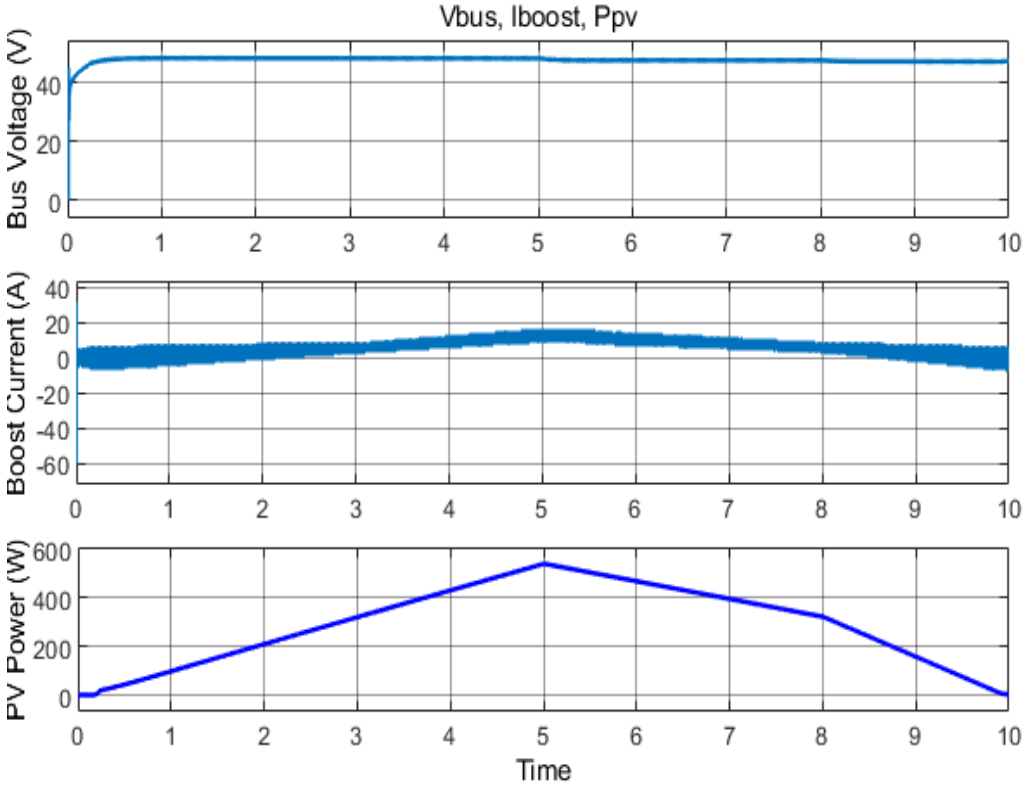

Figure 3.12 Plots for Bus voltage, boost current, output PV power

From Figure 3.11 it is clear that with increase in incident irradiation the current increases rapidly. This increases the power from the solar PV modules and can be seen in Figure 3.12. The bus voltage V_{bus} is maintained constant near about 48V which is similar to the V_{ref} which is also we have taken 48V. Figure 3.13 shows that the outout voltage of the battery across the time (1s) starts increasing from 25.7V. Load of 6Ω is constant.

In Figure 3.13 at t=0s when irradiation is 0W/m^2 the SoC starts decreasing i.e, battery starts discharging. Now as the irradiation is increased to 500W/m^2 at t=4s, the battery current starts decreasing and system becomes unstable for sometime. Now after t=4s irradiation becomes sufficient so that it can charge battery as well as can supply load. Hence battery voltage starts increasing and SoC also starts increasing. At G=1000W/m^2, PV power becomes nearly 1kW. Thus, the performance of the standalone system is studied under irradiance variations. The DC link voltage of the system is well regulated.

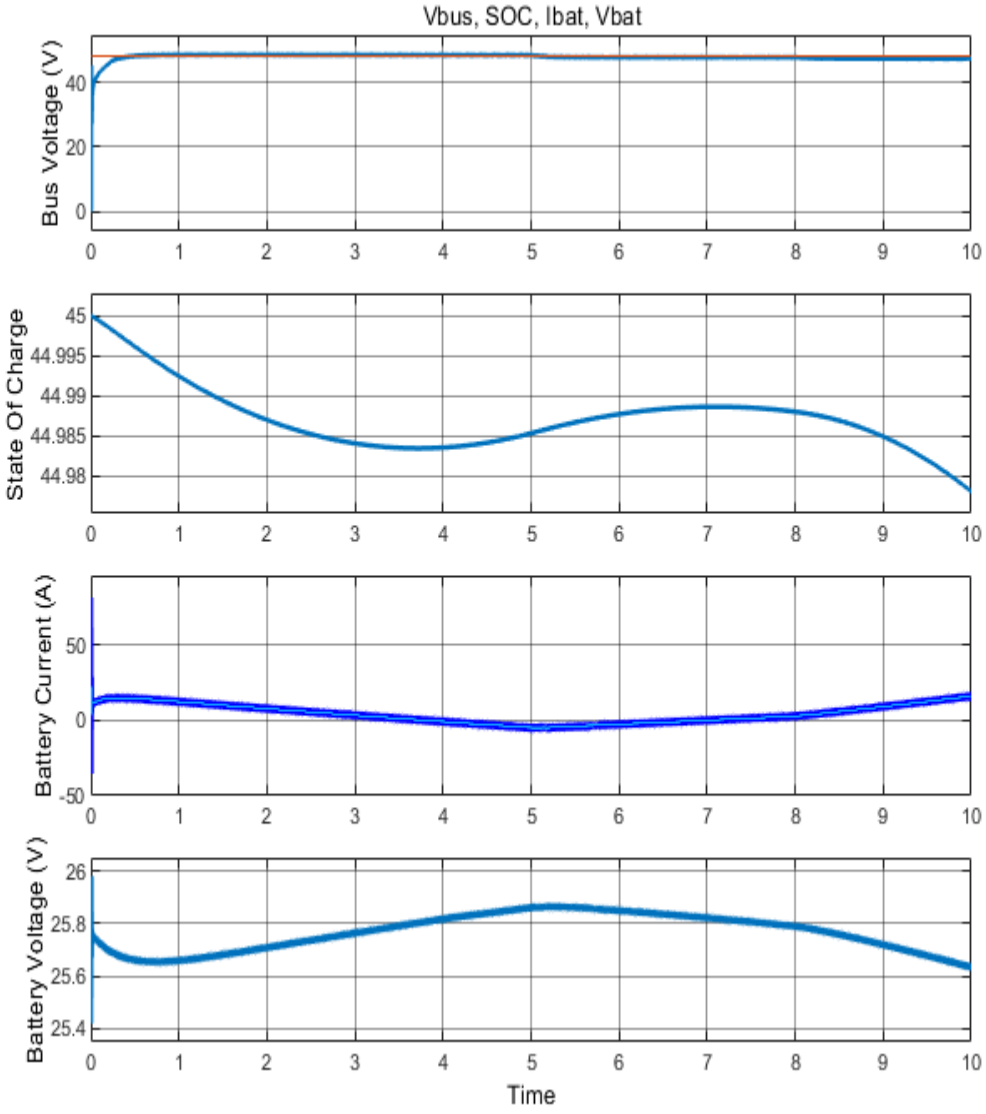

Figure 3.13 Simulation results showing variation of battery parameters wrt time (a) V_{bus} (b)SOC (c)I_{bat} (d)V_{bat}.

3.8 CONCLUSION

In this chapter we saw integration of battery with the photovoltaic panel. This system uses the P&O in the control of MPPT. Whatever the energy is remaining in the battery is taken care by the state of charge (SOC) of the battery. The system charging and discharging takes place based on ambient conditions and load changes.

Therefore 24V lithium-ion battery is charged by the MPPT battery charge controller through tracking the maximum power from the 1kW PV array power source. The presented simulink model can meet any commercial MPPT charge controller by flexible changes with similar topology. So for medium and small standalone PV systems, better sizing of PV panel and battery energy storage is validated by this model.

CHAPTER 4: SINGLE STAGE SINGLE PHASE POWER CONVERSION FOR GRID CONNECTED PV

To transfer efficiently the solar energy in form of irradiation to the utility grid is the main aim of grid-connected photovoltaic (GPV) system. The power conditioning system and solar energy collectors are two parts in which GPV system can be subdivided. The solar energy collectors include PV panels that absorb the solar irradiance coming from the sun and then it is transformed into electrical energy. Maximum amount of energy needs to be extracted from the PV panels, that is the main objective of the power conditioning system. In grid-connected PV system the two primary fields of research is encompassed by these two elements.

4.1 PV CELL MODEL

Using the diode equation behavior of PV cell can be approximated when no light illuminates the PV cell. When there is interaction of the atom of the cell with the incident photons then the electron-hole pairs are produced when the cell is illuminated. A photocurrent is generated by moving of charges and depended mainly on the incident light's intensity and wavelength. With a constant current a PV cell as an ideal p-n junction in parallel is shown in Figure 4.1.

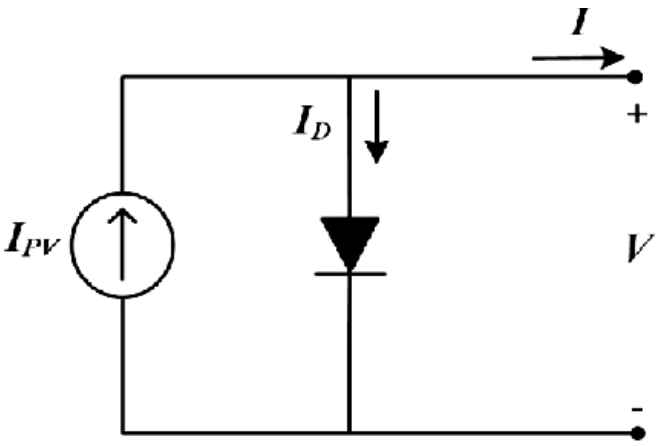

Figure 4.1 Ideal model of PV cell

Light-induced current is represented by I_{PV} and I_D is the diode through current which is derived as

$$I_D = I_{sat}\left[exp\left(\frac{v_{cell}}{\eta V_T}\right) - 1\right] \quad (4.1)$$

where

η = coefficient of emission
I_{sat} = reverse saturation current
V_T = thermal voltage

V_T is given as

$$V_T = \frac{k_B T_{cell}}{q_e} \quad (4.2)$$

where

k_B = Boltzmann constant
q_e = electronic charge
T_{cell} = cell's temperature

Based on the previous equation exponential model of PV cell can be derived:

$$i_{cell} = I_{PV} - I_{sat}\left[exp\left(\frac{v_{cell}}{\eta V_T}\right) - 1\right] \quad (4.3)$$

4.1.1 POWER CONDITIONING SYSTEM

The grid-connected photovoltaic inverter also referred as power conditioning system represents the interface that in which the group of PV panels are connected electrically with the utility grid. So in order that from the PV generator the maximum power must be extracted and to deliver it efficiently to the utility grid is the primary objective of the power conditioning system. Following are the main functional objectives of the power conditioning system.

1. From the PV generators the maximum power must be extracted that is achieved with the help of power converter stage which assures tracking if the point varies.

2. High efficiency power conversion must be achieved which requires the high efficiency power converter.

3. Extracted PV power must be transferred in the appropriate conditions. To accomplish this power conditioning system must make sur that:

    - The grid voltage must be in phase with the current injected into the utility grid. We know that by unity power factor one achieves maximum active power transfer.
    - With the respective standards the injected current harmonic content must comply.
    - DC-AC power conversion must be achieved
    - Power should be flowing from the PV generators to the utility grid.

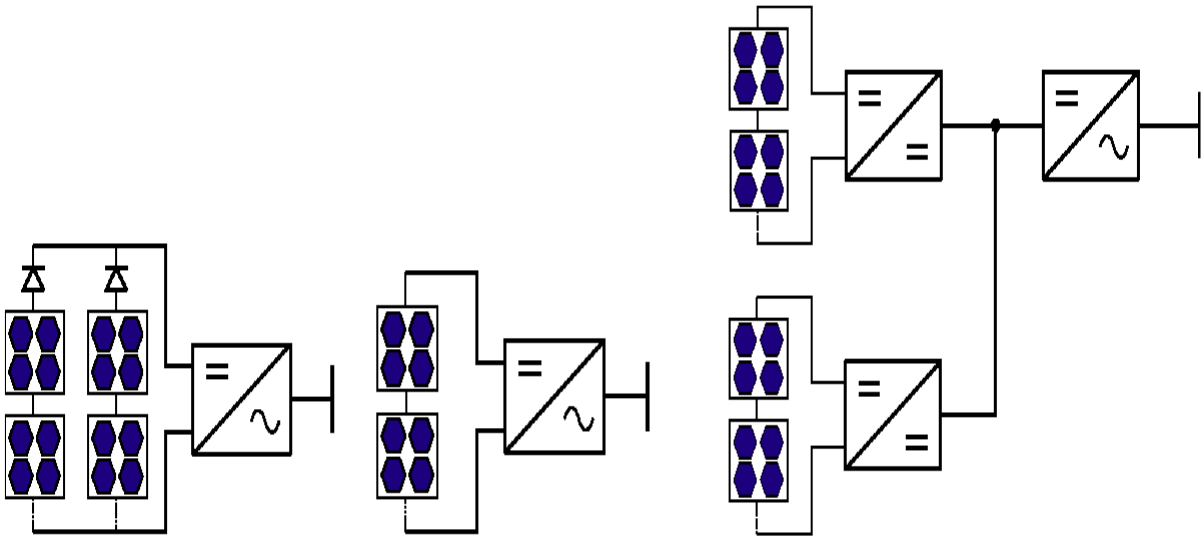

Figure 4.2 (a) Centralized inverter (b) String inverter (c) Multistring inverter

4.2 PROPOSED CONTROL SCHEME FOR THE SYSTEM

The scheme consists of modules namely maximum power point tracker (MPPT), a pulse-width modulation (PWM) and a controller. External variables affect the electrical behaviour of the PV generator since the PV array parameters are unknown, so we need MPPT.

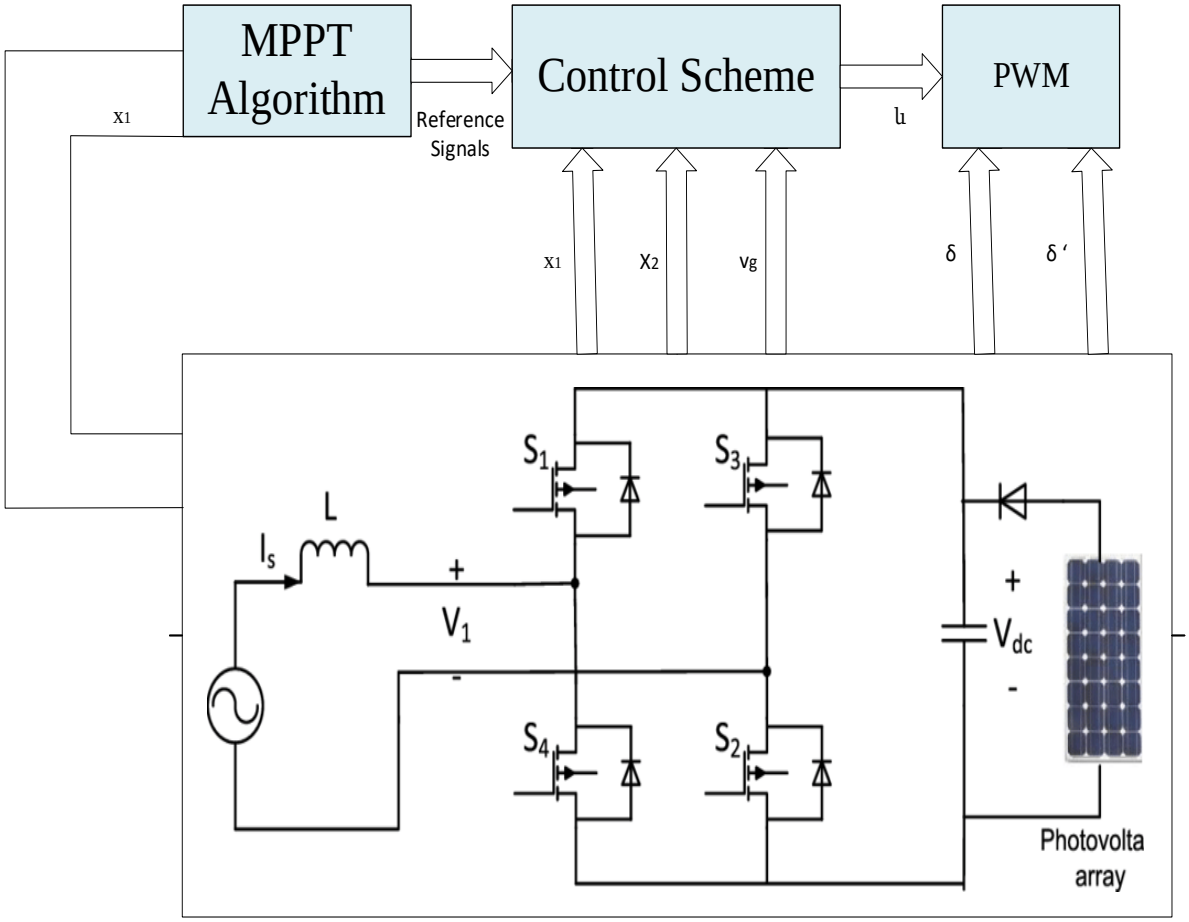

Figure 4.3 Proposed control scheme for single-stage single phase grid connected PV system

Time is in the order of seconds or even minutes for the change of the PV generator electrical characteristics. Referring to the control scheme in Figure 4.3 the power conditioning system's controller uses reference signals generated by MPPT until maximum power extraction is achieved in order to extract different levels of power from the PV array. Lastly the switching signals are generated by the PWM from the duty cycle given by the controller for the full-bridge inverter. Desired reference values can be set with the help of maximum power extraction values but this won't reflect the real behaviour of the GPV system when a MPPT is used i.e. till the maximum power extraction is reached MPPT keeps changing the reference values of the GPV inverter. Control algorithms include dc link voltage control, grid angle detection algorithm, grid current control algorithm and the MPPT algorithm.

4.2.1 DC-LINK VOLTAGE CONTROL

The actual capacitor voltage and the capacitor reference voltage is received by the PI controller to generate the peak value of the current reference that should be injected into the grid by the MPPT block the so that capacitor voltage can be maintained by tracking the reference value generated.

4.3 SYSTEM DESCRIPTION

PV array has a single parallel string each comprising of 11 modules in series and model is capapble of generating power of 2kW as shown in Figure 4.3. The PV module characteristics are given in Table 4.1. The single phase IGBT inverter is connected acoss the dc terminals of the array across a dc capacitor of 600μF through the contactor. Controller starts charging the capacitor by connecting the dc link of the inverter to the PV array. For a reason the controller delays the connection of the grid to the inverter intentionally for a predefined period i.e. to prevent charging the capacitor from the grid. Through a pre-charging resistance the capacitor is pre-charged from the PV array to limit the inrush charging dc current to an acceptable limit. Table 4.2 specifies the specification of system.

Table 4.1 PV module specifications

Short circuit current denoted by I_{SC}	5.5 A
Open circuit voltage denoted by V_{OC}	44.86 V
Current at maximum power point denoted by I_{MPP}	5.04 A
Voltage at maximum power point denoted by V_{MPP}	37.73 V
Number of cells in series denoted by N_S	72
P_{MAX}	190.15W

Table 4.2 System specifications

V_{op}	312V
P	4.5kW
f_{sw}	5kHz
ΔI	5% of 14A=0.7A
ΔV	1% of 230=2.3V
I_{op}	4.5kW/312V=14A
V_{oc}	44.86V
V_{mppt}	493.5V
V_{dc}	410V
C_{PV}	600μF
L_{filter}	4.06mH
C_{filter}	6.23μF

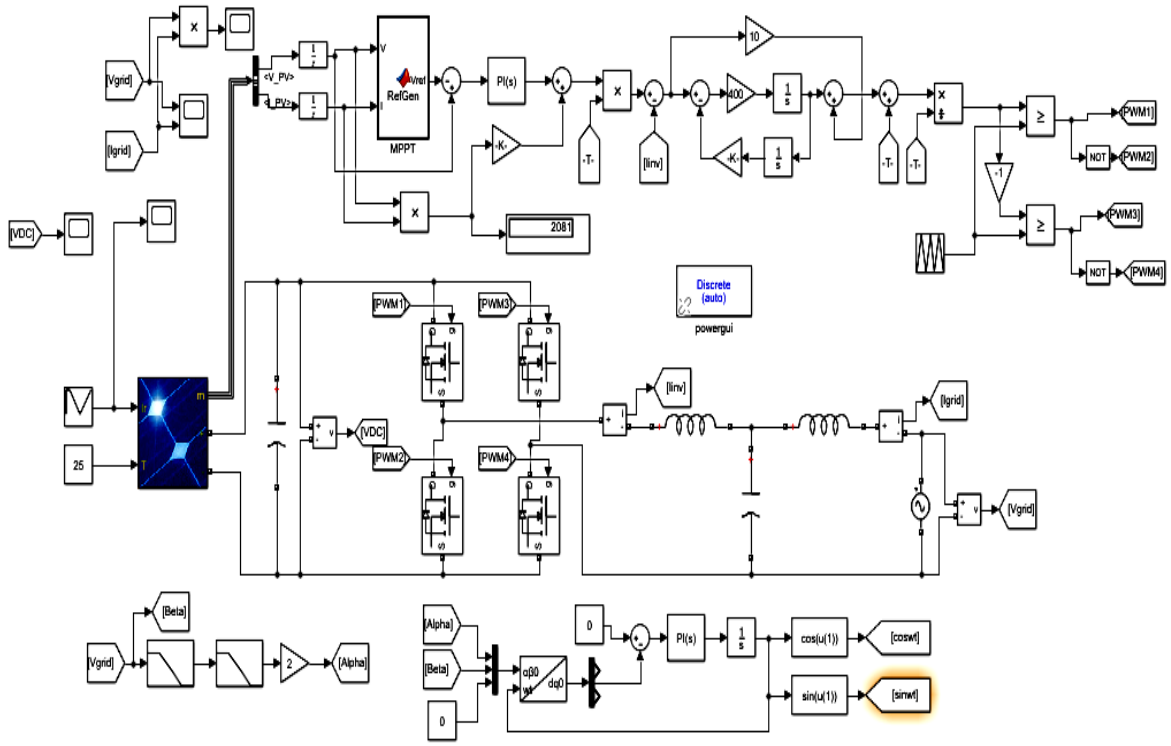

Figure 4.4 Model showing the overview of single stage single phase grid connected pv system

4.4 MPPT ALGORITHM

The proposed MPPT flowchart is shown in Figure 4.5. To set up a fixed voltage whose value is 0.8 times of the PV array open-circuit voltage is the first step. Then using the saved previous voltage and current the d-axis grid current and the PV array instantaneous voltage are measured in order to calculate the differential values of current. For obtaining MPP an iterative method can be Perturb & Observe method. With respect to the voltage when the rate of change of power is zero the maximum point is reached.

The process is repeated periodically until the MPP is reached and this is the major drawback of the conventional P&O method. Then about MPP the system oscillates. If the perturbation step size is reduced then the oscillation can be minimized. Yet MPPT is slowed down by a smaller perturbation size. Here two step sizes d1 and d2 are used where d1>d2. If dP/dV is positive the direction should be same in which increment is with the direction in perturbation of the operating voltage is.

When the error E = P'(r) – P'(r-1) is large, to have a fast tracking of MPP the algorithm selects the step size as K=d_1. Based on the tracking time of MPP the exact value of d_1 is chosen. The step size d_2 is chosen as 1/10 times of k_1 to minimize the power ripple. Having the same phase angle, frequency and amplitude between the PV inverter and the grid means that both are synchronized. On the PI block parameters depends the time required for the synchronization.

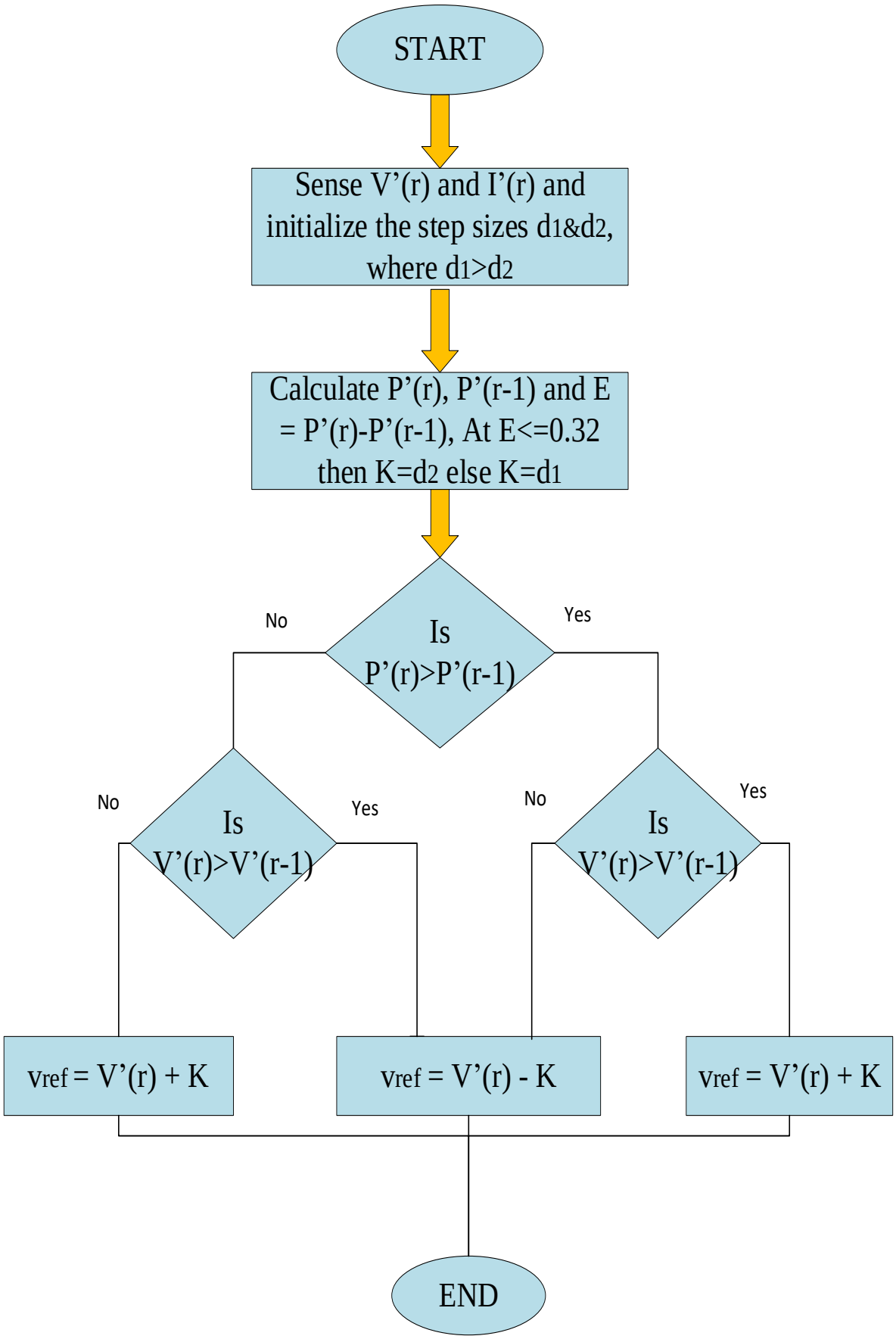

Figure 4.5 MPPT flowchart for the proposed system

4.5 SIMULATION RESULTS

Various system parameters like voltage and current are measured. The simulation of the PV module is done when irradiation is varied (0-1000 W/m^2) and when temperature is constant at 25˚C. In the case I the irradiation is varied and temperature is kept constant at 25˚C. The voltage and grid current is shown in Figure 4.6. A decrease in magnitude of the current can be clearly seen from 0.5s to 2s during which irradiation decreased from 1000 W/m^2 to 300 W/m^2 and then again starts increasing till 3.5s.

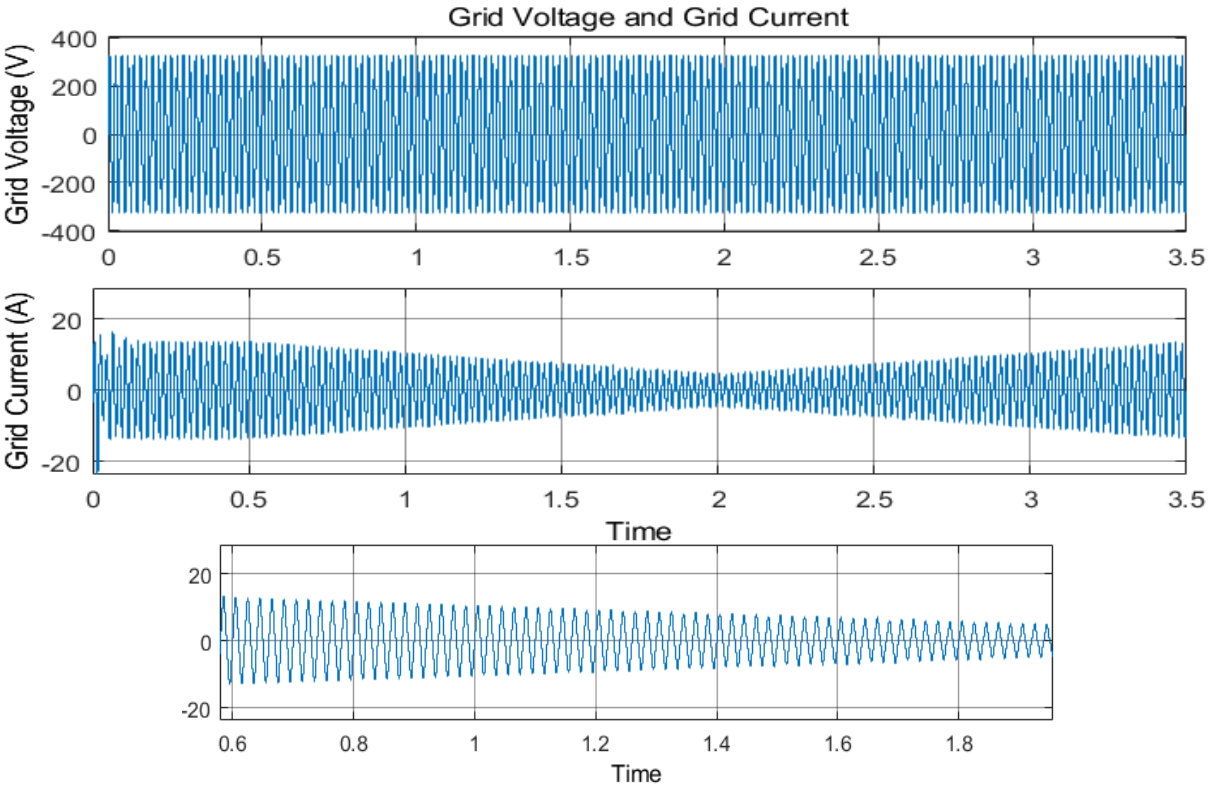

Figure 4.6 Voltage and Current of the grid when irradiation is varied

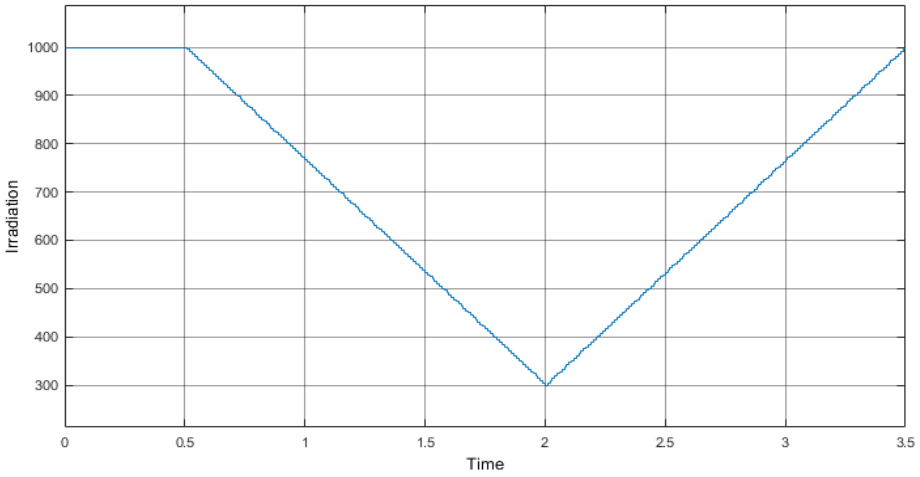

Figure 4.7 Variation of the irradiation

In case II irradiation is made 700 W/m^2 at 0.5s then slightly increases to 800 W/m^2 till 1.5s and then starts decreasing till 2.5s to 400 W/m^2 and then finally reaches to 1000 W/m^2 at the end of 3.5s. The variation of the grid current when irradiation is decreasing and increasing between 2s to 3.5s can be seen in Figure 4.8. Irradiation is seen in Figure 4.9. Grid voltage is maintained constant at 330V and grid current varies with respect to irradiation.

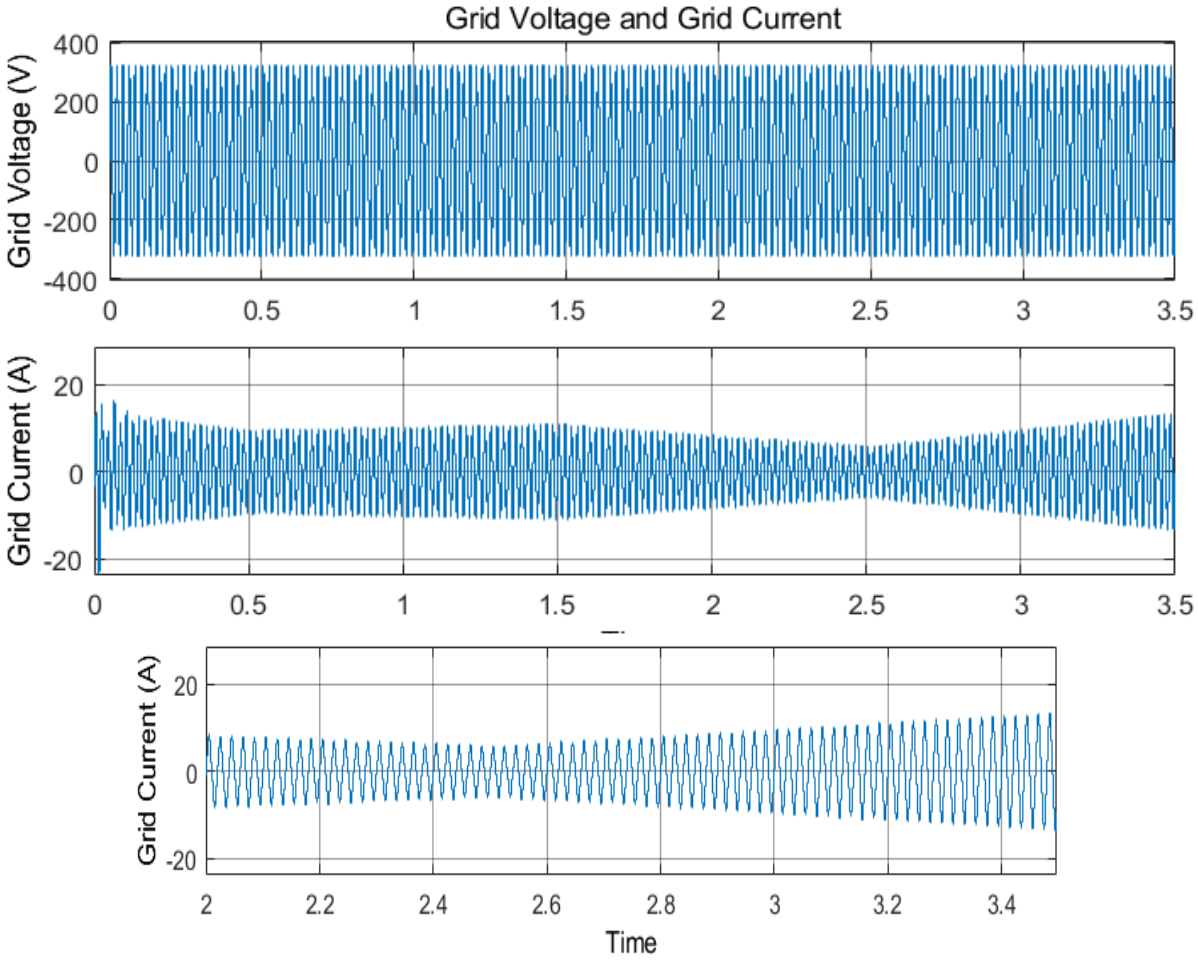

Figure 4.8 Voltage and Current of the grid when temperature is varied

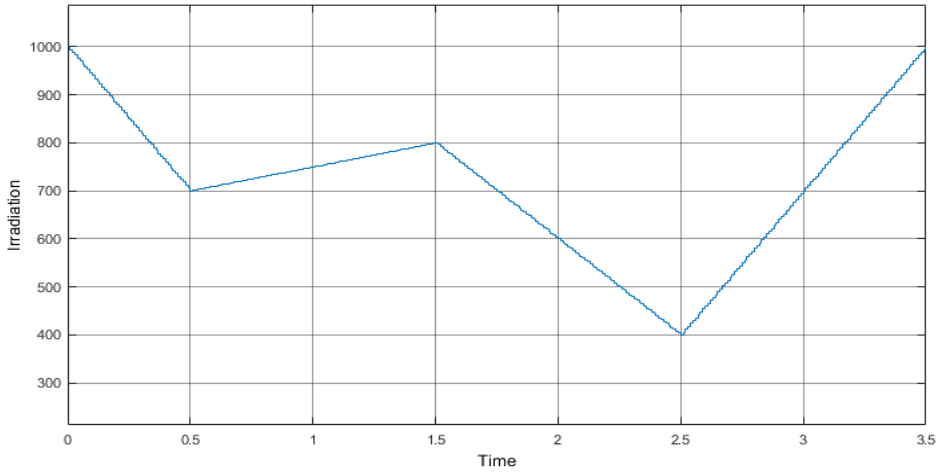

Figure 4.9 Variation of the irradiation

4.6 CONCLUSION

In this chapter 4 the proposed control system gives a clarity over the strategy how to deliver the maximum power to the grid and how to track the maximum power. Two different modes of operation i.e, when irradiation is varied and other when temperature is varied are tested by the grid connected PV system. Perturb & Observe based MPPT controller have been used for optimum use of PV module. The system shown works satisfactorily under all conditions.

In chapter 4 single-stage single phase converter was simulated and the advantages of the single-stage converter are good efficiency, a lower price and easier implementations and one major disadvantage is that if shading occurs on one or more PV panels then the efficiency of the whole system is reduced.

CHAPTER 5: PERFORMANCE ANALYSIS OF BIDIRECTIONAL BATTERY CHARGER FOR EV

To encourage the growth of vehicle to grid technology, a vital role has been played by the increase in the electric vehicle mobility. In this chapter vehicle-to-grid (V2G) and grid- to-vehicle (G2V) technologies are developed. When V2G mode is operated the power grid are delivered back the energy stored in batteries and during G2V mode operation batteries are charged from the power grid. To preserve the power quality in the power grids EVs battery charging process must be regulated. The interactivity of EVs with the smart grid. EVs can also be used to feed the home loads as they can operate as voltage source beside the V2G and G2V operation. Thus, first step to the smart grid evolution will be the smart homes with energy management and efficiency solutions. A bi-directional battery is designed in this chapter which the power grid recives the energy (G2V), and then the energy is delivered back to the power grid which is stored as a part of energy in the batteries (V2G). Bidirectional battery charger technology implemented in this chapter is shown by the block diagram in Figure 5.1.

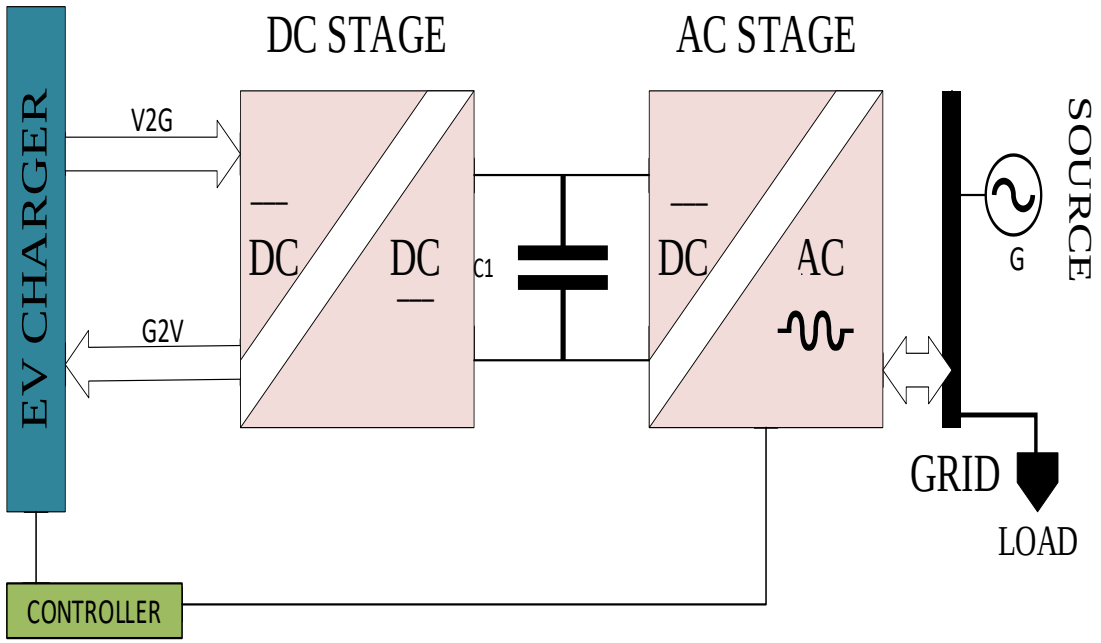

Figure 5.1 Block Diagram for Bidirectional Battery Charger Technology

5.1 EV CHARGING DESIGN

Since 1868, the history of electric vehicle started and to utilize EV as future vehicle since then studies were going on. Wherever the distribution grid is integrated with EV the place is called EV charging station. To ensure a quality grid integration while designing the components in the charging station expert care has to be given. A lot of challenges in power quality is seen when integration of EV with the grid is done. Constant voltage/constant current strategy is employed in the DC-DC converter that helps in EV battery charging/discharging. The charging station rated capacity can be described from the equation given below-

$$S_{rated} = \frac{K_{LOAD} N_{SLOT} P_{EV}}{cos\emptyset}\ kVA \quad (5.1)$$

where

K_{load} = overload factor depended on the charging station rated capacity
N_{slot} = number of slots provided
P_{EV} = individual maximum power
cosϕ = power factor

DC bus nominal voltage upper limit is calculated as

$$V_{dc} = \frac{V_{bat}^{min}}{m_{min}}\ Volts \quad (5.2)$$

where V_{bat}^{min} = minimum battery voltage

m_{min} = minimum modulation index

5.1.1 DC BUS CAPACITOR [34]

The stability of the DC bus is determined by the size of the DC capacitor. We need a DC bus capacitor for high ripple currents. The value of DC capacitor is calculated as-

$$C_{dc} = \frac{S_{rated}}{V_{dc}^2} \frac{2nT\Delta P_{dc} cos\emptyset}{\Delta V_{bus}}\ Farad \quad (5.3)$$

where T = time period
ΔP_{dc} = allowable dc power
ΔV_{bus} = bus voltage

5.1.2 BATTERY SELECTION OF EV [34]

Lithium-Ion battery is the most commonly used EV battery yet Nickel-Cadmium batteries are also used. Ampere hour capacity, life of the battery, cut-off voltage, nominal energy, internal resistance, nominal voltage, etc are some specifications.

5.1.3 BATTERY CHARGER UNIT OF EV [34-38]

Battery charger unit with buck boost battery charger is shown in Figure 5.2

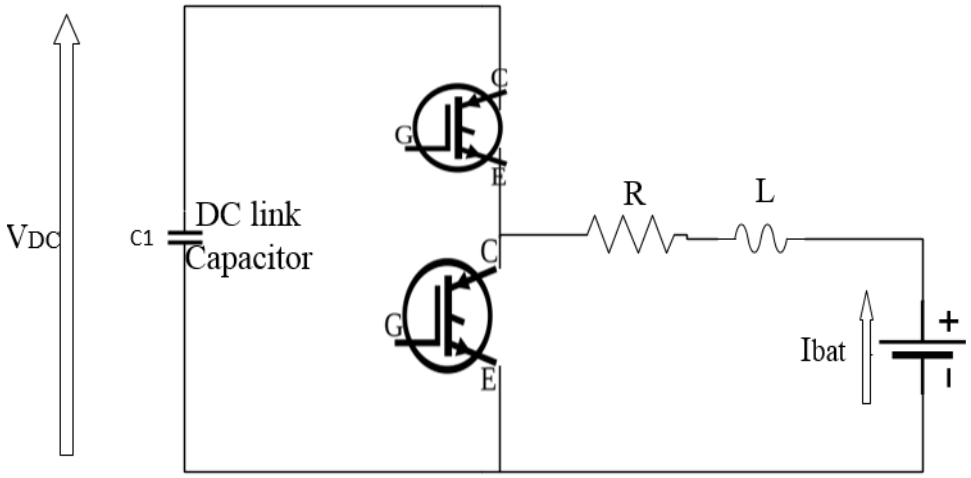

Figure 5.2 Battery charger unit

The buck and boost mode operation are performed by two IGBT switches under the required control strategy. DC-DC converter is served by this unit.

5.1.4 THREE PHASE CONVERTER [34-38]

The AC-DC converter controls the power exchange between AC grid and the DC converter. When gate pulses are fed to the converter switches which are of IGBT type to control its operation and it is a type of bidirectional converter. Figure 5.3 represents the three phase converter unit for the system.

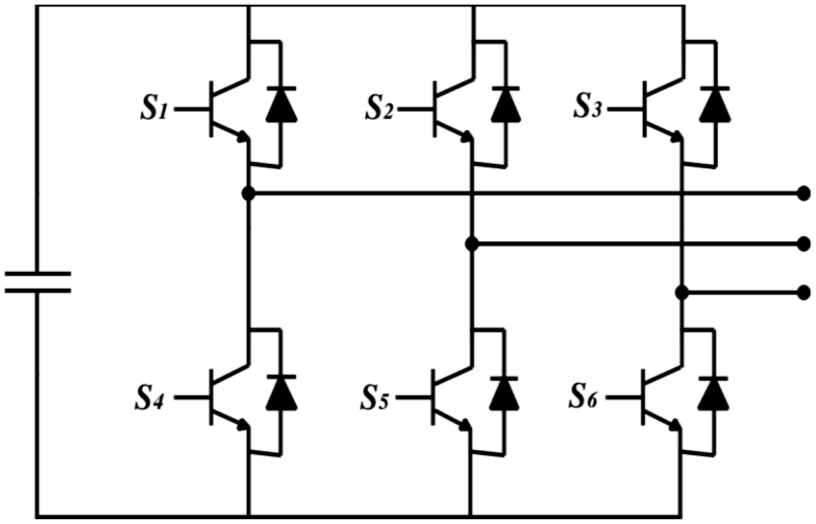

Figure 5.3 Three phase converter unit

5.1.5 LCL FILTER [38]

To cut out the harmonics in the system we need filters. Figure 5.4 shows the filter which is made up of inductor of converter side (L_2) and filter capacitor (C_f) and inductor of grid side (L_1).

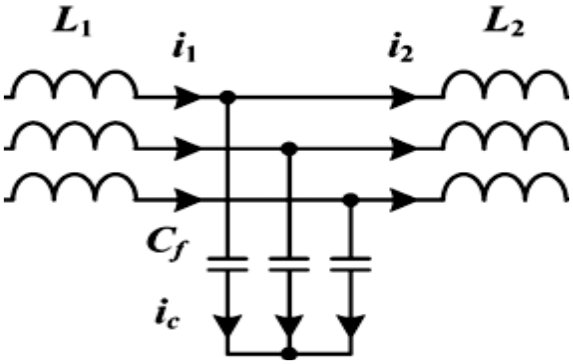

Figure 5.4 LCL filter representation

where

$$L_2 = \frac{V_{grid}^2 \sqrt{\frac{\pi^2}{18}\left(\frac{3}{2} - \frac{4\sqrt{3}}{\pi} m_a + \frac{9}{8} m_a^2\right)}}{S_{rated} . THD . 2\pi f_{SW}} \; H \tag{5.4}$$

$$C_f \leq \frac{0.05 S_{rated}}{2\pi . \, f_{grid} . \, V_{grid}^2} \; F \tag{5.5}$$

$$L_1 = \frac{RAF+1}{RAF\,.\,C_f\,.\,2\pi f_{SW}^2}\,\text{H} \tag{5.6}$$

where f_{SW} = switching frequency
f_{grid} = grid frequency
m_a = modulation index
RAF = ripple attenuation factor

Table 5.1 EV battery parameters

Parameters	Specifications
Battery Type	Lithium-Ion
Nominal Voltage	360V
Initially SOC	50%
Ampere Hour Rating	300Ah
Fully Charged Voltage	419.03V
Cut-off Voltage	270V
Nominal Discharge Current	130.43A

5.2 CONTROLS USED

A smooth transition from the grid to voltage mode to voltage to grid mode is provided by the control system and simultaneous EV charging and discharging is provided. To control the inverter operation, dq reference frame control method is implemented. Voltage loops and current loops are connected in cascaded structure in it. Alternating current, DC bus voltage and the active & reactive power are controlled by the controller. Figure 5.5 shows the inverter control in d-q frame.

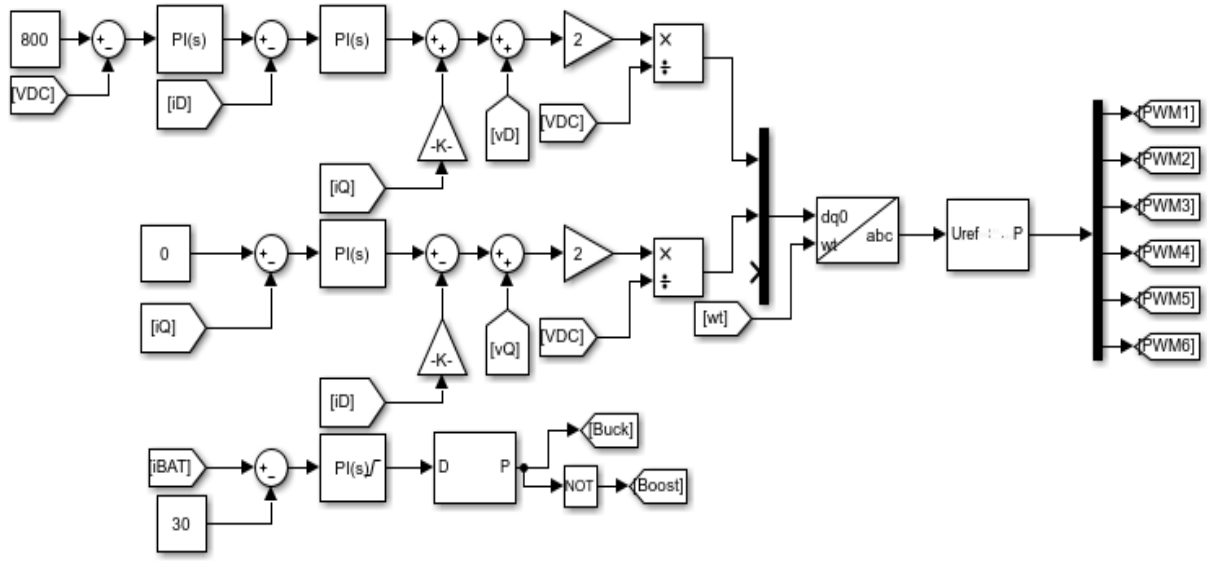

Figure 5.5 Inverter control in d-q frame

Using a PLL block, grid synchronization has been made possible shown in Figure 5.6. Input of the PLL block is provided with the measured three-phase voltage. Separate control strategies are implemented for charging. Simulink model for the EV charging system is shown in Figure 5.7.

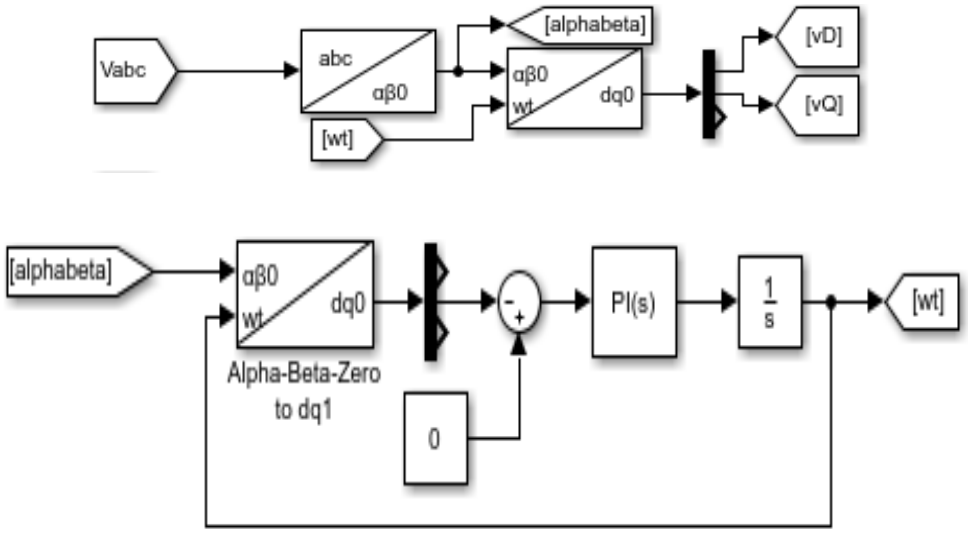

Figure 5.6 PLL block diagram

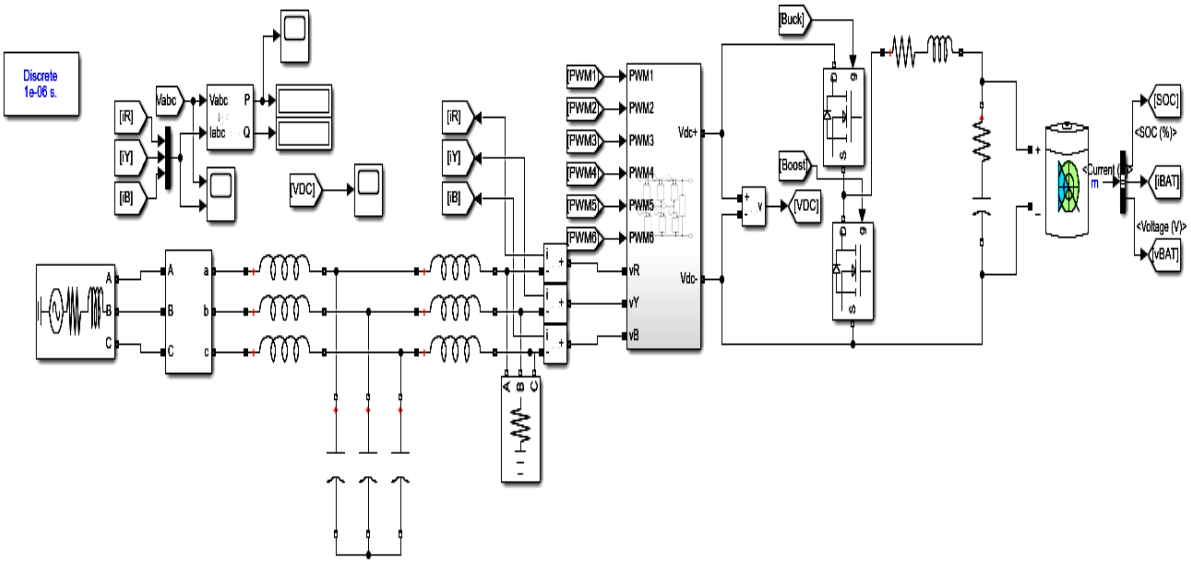

Figure 5.7 Simulink model of the system

In constant current strategy, the converter will operate in boost mode (discharging process) as the battery operates as a constant current source whereas in constant voltage strategy, the converter will operate in buck mode (charging process) as the battery charges under a constant voltage source. Somewhat slightly greater than the peak value would be the DC link voltage of the power grid voltage in order such that the full-bridge AC-DC bidirectional converter deliver back the energy to the power grid stored in the traction batteries. During short time periods, any significant variation is not suffered by the batteries voltage so that by the absorption of the constant current from the batteries.

.The error between the actual current and the reference current feeds a PI controller that adjusts the duty-cycle for a 10kHz PWM modulator.

5.3 SIMULINK RESULT

To test the performance of the proposed bidirectional controller under grid to vehicle and vehicle to grid operation this simulation is conducted. The SOC of the battery is set initially to 50%. This value is selected so that the battery is able to supply or receive power when necessary. Two cases are considered Case I for vehicle to grid mode and Case II for grid to vehicle mode.

Case I: SOC starts decreasing gradually from 50%. Value of battery current is positive near abut 30A when battery is discharging. Battery voltage has been decreased slightly from 387.5V to 386.5V and all these can be seen in Figure 5.11. V_{grid} is about 330V that can be seen in Figure 5.8 it needs to be synchronous because we are sending back the power to grid so, the magnitude needs to be in phase and be equal whereas I_{grid} is 22A and can be seen in Figure 5.8. V_{dc} link voltage is constant at 800V after t =0.4s and can be seen in Figure 5.9.

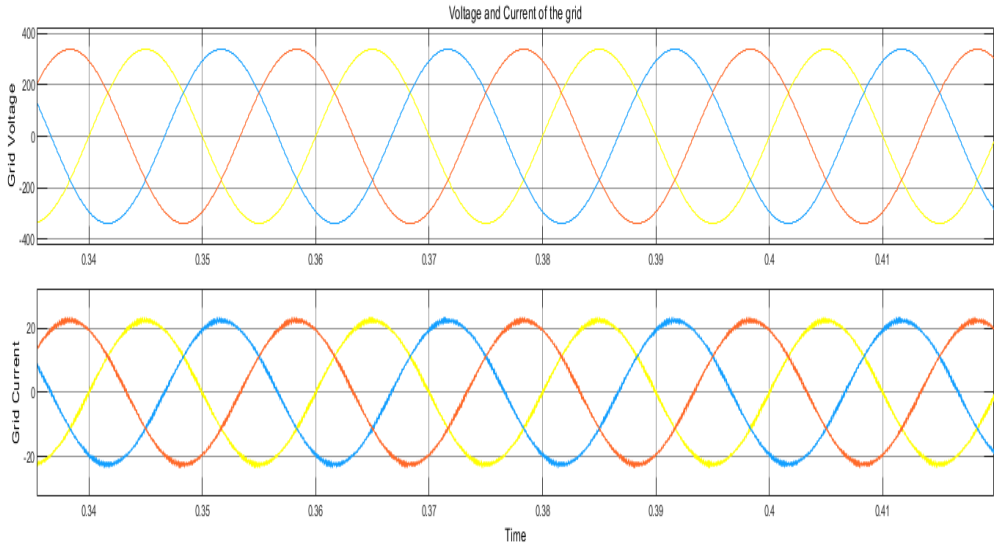

Figure 5.8 Voltage and Current of the grid during V2G mode

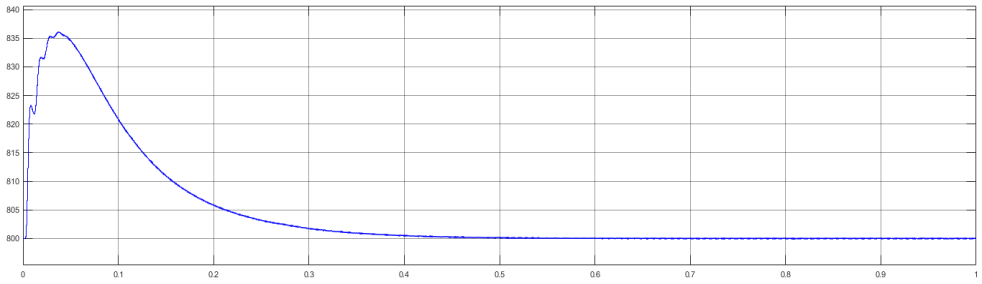

Figure 5.9 V_{dc} link voltage

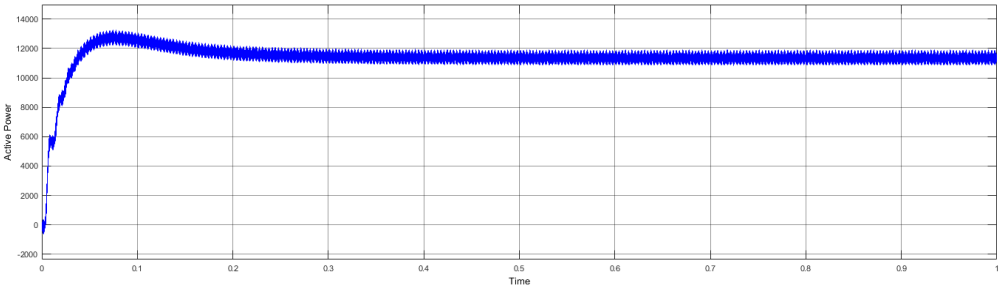

Figure 5.10 Plot for the active power of the system during V2G mode

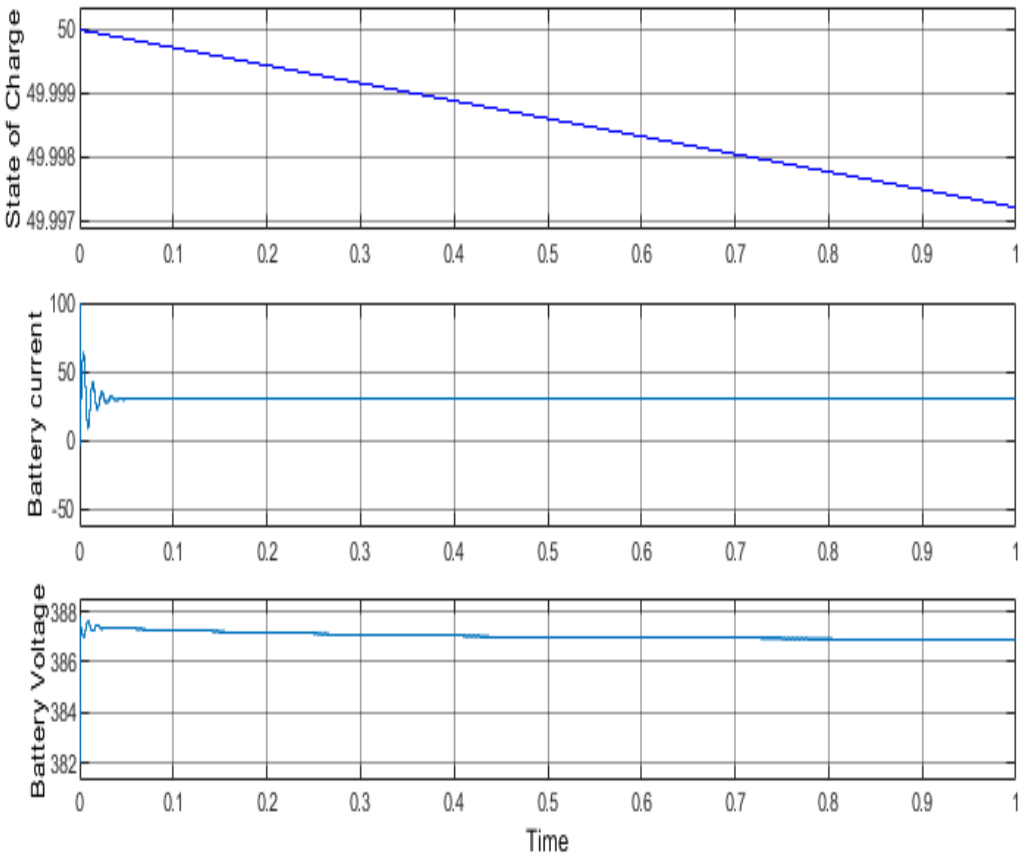

Figure 5.11 SOC, Battery current and Battery voltage for the V2G mode

Case II: In this case SOC starts increasing since the battery is charging from 50%. Value of battery current is negative i.e. -30A. Negative because battery is in charging state. Battery voltage has increased a slight bit from 388V to 388.5V. All these can be observed in the Figure 5.15. V_{grid} is maintained constant at 330V in this case also and can be verified from Figure 5.12 and similarly grid current I_{grid} is 22A. Here we can see a phase difference of 180˚ between the V_{grid} and I_{grid}. Similarly V_{dc} link voltage is maintained about 800V in this case also and this can be verified from Figure 5.13.

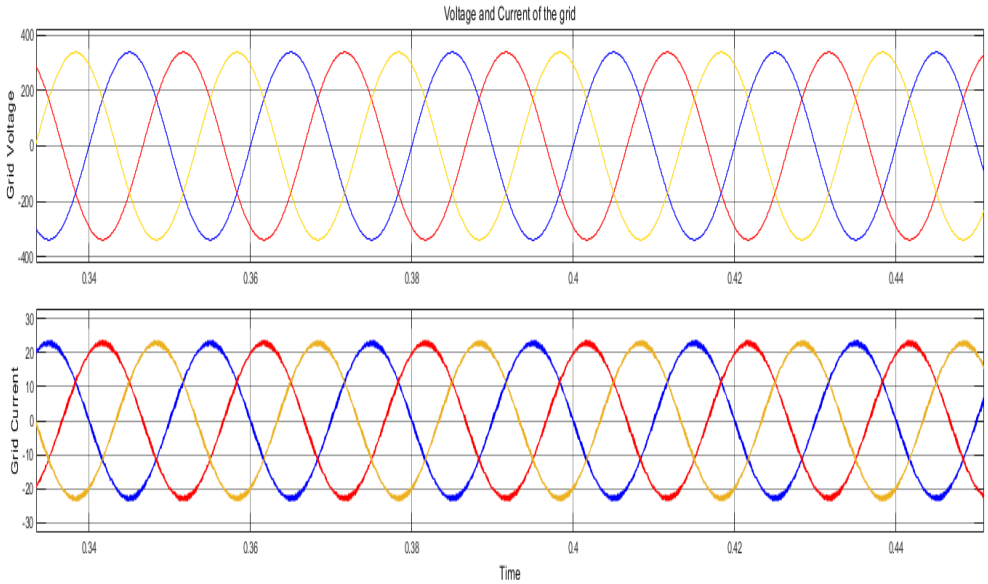

Figure 5.12 Voltage and current of the grid during G2V mode

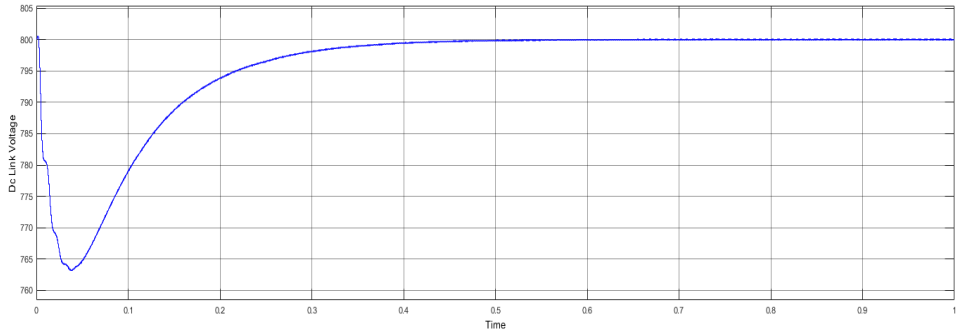

Figure 5.13 V_{dc} link voltage

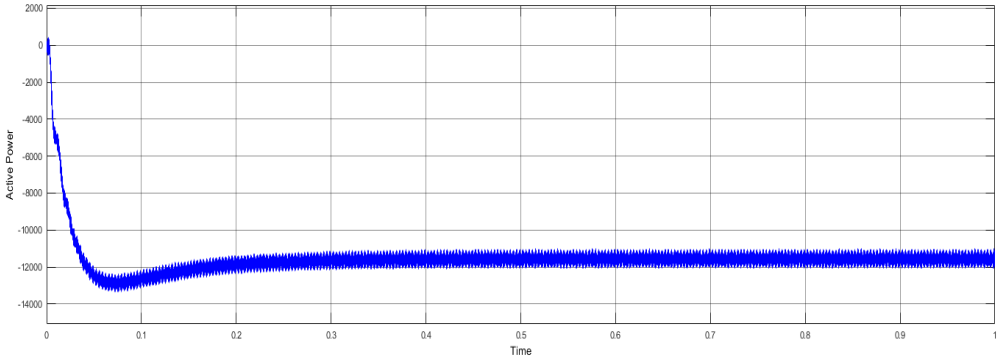

Figure 5.14 Plot for the active power of the system during G2V mode

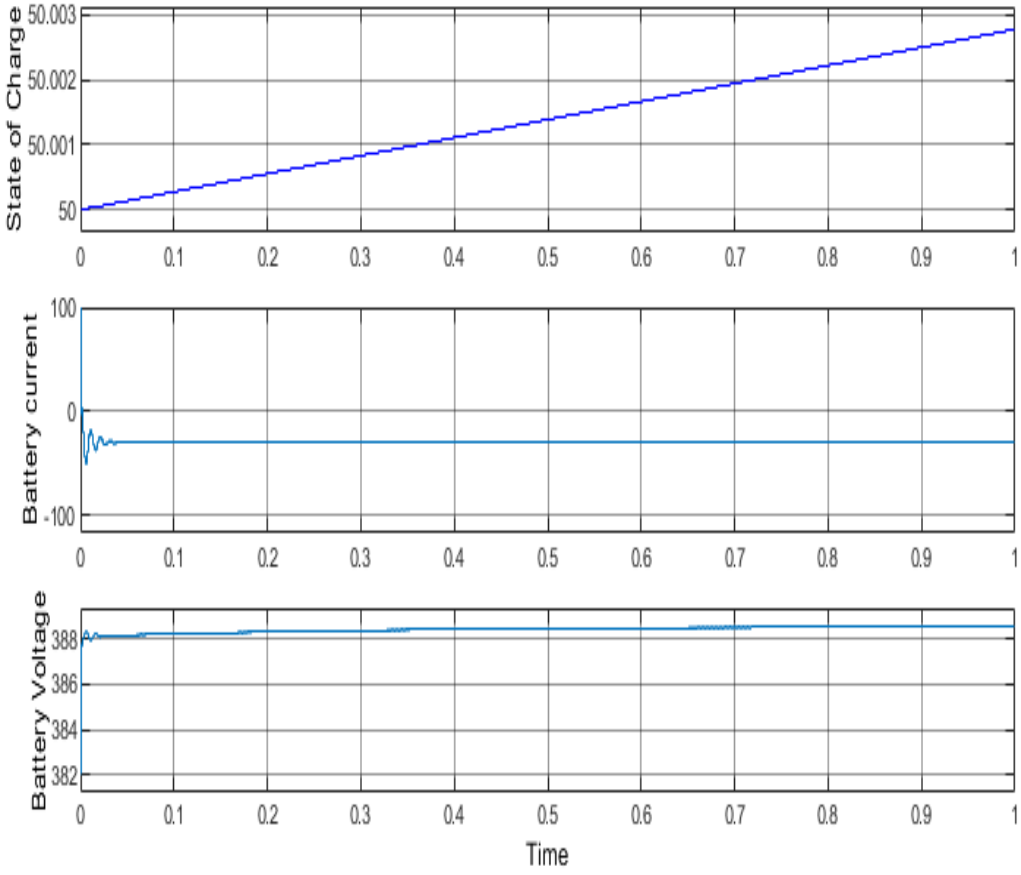

Figure 5.15 SOC, Battery current and Battery voltage for the G2V mode

5.4 CONCLUSION

In the chapter 5 model integrating the EV battery with the grid has been presented. Each element's modeling equation is also explained with MATLAB model implementation. The feasibility of both charging mode and discharging mode is illustrated in the simulation results. A sustained approach is promised by the vehicle to grid mode where environment is also a major concern but due to high initial cost, resistance to change by the people and manufacturers and lack of government subsidy has faced lot of criticism. Vehicle to grid will become a widespread phenomenon when more durable batteries and cost efficient grid lines become common.

REFERENCES

[1] H. Ritchie and M. Roser, "Energy Production & Changing Energy Sources," OurWorldInData.org, 2017. [Online]. Available: https://ourworldindata.org/energy-production-and-changing-energy-sources/. [Accessed November 2017].

[2] REN21, "Renewables 2017 Global Status Report "Market And Industry Trends"," 2017. [Online]. Available: http://www.ren21.net/wp-content/uploads/2017/06/17-8399_GSR_2017_Full_Report_0621_Opt.pdf. [Accessed December 2017].

[3] S. Hegedus and A. Luque, "Achievements and challenges of solar electricity from photovoltaics," in *Handbook of Photovoltaic Science and Engineering*, John Wiley & Sons, Ltd, 2011, pp. 2-38.

[4] G. Dzimano, *Modeling Of Photovoltaic Systems, Doctoral Thesis,* The Ohio State University, 2008.

[5] S. Kjaer, J. Pedersen and F. Blaabjerg, "A review of single-phase grid-connected inverters for photovoltaic modules," *IEEE Transactions on Industry Applications,* vol. 41, no. 5, pp. 1292-1306, Sept.-Oct. 2005..

[6] Villalva, M.G., Gazoli, J.R. and Filho, E.R.; "Modeling and circuit-based simulation of photovoltaic arrays," *Power Electronics Conference, IEEE 2009. COBEP '09. Brazilian*, December 2009, pp. 1244 - 1254.

[7] Zhou Dejia, Zhao Zhengming, Eltawil, M. and Yuan Liqiang; "Design and control of a Three-phase Grid connected Photovoltaic system with developed Maximum power point tracking,"*Applied Power Electronics Conference and Exposition, 2008. APEC 2008. Twenty-Third Annual IEEE,* May 2008, pp. 973 - 979.

[8] Azevedo, G.M.S., Cavalcanti, M.C., Oliveira, K.C., Neves, F.A.S. and Lins, Z.D., "Evaluation of maximum power point tracking methods for grid connected photovoltaic systems," Conference on *Power Electronics Specialists, 2008. PESC 2008. IEEE* , August 2008, pp. 1456 - 1462.

[9] Weiping Luo and Gujing Han, "Tracking and controlling of maximum power point application in grid-connected photovoltaic generation system," *Second International Symposium on Knowledge Acquisition and Modeling 2009, KAM '09,* vol. 3, December 2009, pp. 237 - 240.

[10] S. M. I. Jeyraj Selvaraj and Nasrudin A. Rahim, "Multilevel Inverter For Grid-Connected PV System," *IEEE Transactions on Industrial Electronics,* vol. 56, pp. 149-158, 2009.

[11] "What's inside a solar panel?," 12 April 2012. [Online]. Available: http://solarphotovoltaic.blogspot.com/.

[12] F. Z. L. M. T. O. A. Amatoul, "Design Control of DC/AC Converter for a Grid Connected PV Systems with Maximum Power Tracking Using MATLAB/SIMULINK,," in *International Conference on Multimedia Computing and Systems*, Ouarzazate, 2011.

[13] Liang Ma, Wang Ran and Zheng, T.Q., "Modeling and Control of 100 kW Three-phase grid-connected Photovoltaic inverter," *Industrial Electronics and Applications (ICIEA), 2010 the 5th IEEE Conference*, July 2010, pp. 825 - 830.

[14] Calais, M. and Agelidis, V.G., "Multilevel Converters fo Single-phase grid connected photovoltaic Systems – An overview," *IEEE International Symposium on Industrial Electronics, 1998. Proceedings. ISIE '98,* vol. 1, August 2002, pp. 224 - 229.

[15] "Ralph J. Brodd, "Synopsis of the Lithium-Ion Battery Markets"," in *Lithium-Ion Batteries, Science and Technologies*, Springer, 2009, p. 2.

[16] G. Blomgren, R. Powers and D. MacArthur, "Lithium and Lithium Ion Batteries," 2002.

[17] X. Hu, S. Li, H. Peng and F. Sun, "Robustness analysis of State-of-Charge estimation methods for two types of Li-ion batteries,," *Journal of Power Sources,* vol. 217, pp. 209-219, November 2012.

[18] D. Linden and T. B. Reddy, "Chapter 23 - lead-acid batteries," in *Handbook of Batteries*, McGraw-Hill, 2002.

[19] A. A. M. U. YAGMUR KIRCICEK, "Modeling and Analysis of a Battery Energy Storage System," in *7th International Ege Energy Symposium & Exhibition*, Usak , 2014.

[20] E. Koutroulis and K. Kalaitzakis, "Novel Battery Charging Regulation System for Photovoltaic Applications", *IEEE Proceeding - Electric Power Applications,* 151, 2004, pp. 191-197.

[21] J. D. Wang and F. Yang, "Optimal capacity allocation of standalone wind/solar/battery hybrid power system based on improved particle swarm optimization algorithm" IET Renewable Power Generation vol. 7 no. 5, 2013, pp. 443- 448.

[22] M. a. M. R. G. A. Chen, "Accurate electrical battery model capable of predicting runtime and I-V performance," *IEEE Transaction on Energy Conversion,* vol. 21, pp. 504-511, 2006.

[23] P. a. V. K. Garg², "To Perform Matlab Simulation of Battery Charging Using Solar Power With Maximum Power Point Tracking(MPPT)," *International Journal of Electronic and Electrical Engineering*, vol. 7, pp. 511-516, 2014.
[24] W.-Y. Chang, "The State of Charge Estimating Methods for Battery: A Review," *ISRN Applied Mathematics*, vol. 2013, p. 7, 2013.
[25] M. a. R.-M. G. A. Chen, "Accurate electrical battery model capable of predicting runtime and I-V performance," *IEEE Transaction on Energy Conversion*, vol. 21, pp. 504-511, 2006.
[26] M. Ciobotaru, R. Teodorescu and F. Blaabjerg, A new single-phase PLL structure based on second order generalized integrator, Record of IEEE PESC 2006, Korea, p. 1511-1516.
[27] M. H. Rashid, Power Electronics Handbook, Third, Ed., Butterworth-Heinemann pu, 2011.
[28] Calais, M., Myrzik, J., Spooner, T. and Agelidis, V.G., "Inverters for single-phase grid connected photovoltaic systems – an overview," *Power Electronics Specialists Conference, 2002. pesc 02. 2002 IEEE 33rd Annual*, vol. 4, November 2002,pp. 1995 - 2000.
[29] Jain, S. and Agarwal, V., "A single-stage grid connected inverter topology for solar PV systems with maximum power point tracking," *IEEE Transactions on Power Electronics*, vol. 22, September 2007, pp. 1928-1940.
[30] Gonzalez, R. Lopez, J. Sanchis, P. Marroyo, L, **"**Transformerless Inverter for Single-Phase Photovoltaic Systems", ,*IEEE Transaction in Power electronics 2007 volume 22 issue 2*, page 693-697.
[31] Esram, T. and Chapman, P.L., "Comparison of Photovoltaic array maximum power point tracking techniques," *IEEE Transactions on Energy Conversion*, vol.22, May 2007, pp.439 - 449.
[32] C. K. L. C. Z. a. W. G. H. M. Coleman, "State-of-charge determination from EMF voltage estimation: using impedance, terminal voltage, and current for lead-acid and lithium-ion batteries," *IEEE Transactions on Industrial Electronics*, vol. 54, p. 2550–2557, 2007.
[33] A. Shukla, K. Verma, and R. Kumar, "Impact of EV fast charging station on distribution system embedded with wind generation," *J. Eng.*, vol. 2019, no. 18, pp. 4692–4697, 2019, doi: 10.1049/joe.2018.9322.
[34] Y. Huang, J. J. Ye, X. Du, and L. Y. Niu, "Simulation study of system operating efficiency of EV charging stations with different power supply topologies," *Appl. Mech. Mater.*, vol. 494–495, pp. 1500–1508, 2014, doi: 10.4028/www.scientific.net/AMM.494-495.1500.
[35] D. Sbordone, I. Bertini, B. Di Pietra, M. C. Falvo, A. Genovese, and L. Martirano, "EV fast charging stations and energy storage technologies: A real implementation in the smart micro grid paradigm," *Electr. Power Syst. Res.*, vol. 120, pp. 96–108, 2015, doi: 10.1016/j.epsr.2014.07.033.
[36] http://www.sae.org/smartgrid/chargingspeeds.pdf.Arancibia A., Strunz K., "Modeling of electric vehicle charging station for fast DC charging" Electric Vehicle Conference (IEVC), 2012 IEEE International.Karlsson P. Svensson J., "DC bus voltage control for distributed power systems", Power Electronics, IEEE Transaction on Vol.18, no.6, pp. 1405-1412, nov 2003.
[37] W. Kempton, J. Tomic, S. Letendre, A. Brooks and T. Lipman, "Vehicle-to-grid power: battery, hybrid, and fuel cell vehicles as resources for distributed electric power in California", UCD-ITS-RR-01-03, June 2001.
[38] W. Kempton and V. Udo, Ken Huber, K. Komara, S. Letendre, S. Baker, D. Brunner and N. Pearre, "A test of vehicle-to-grid (v2g) for energy storage and frequency regulation in the PJM system", nov. 2008.
[39] E. Sortomme, "Combined bidding of regulation and spinning reserves for unidirectional vehicle-to-grid," IEEE PES Innovative Smart Grid Technologies, Washington, DC, 16-20 Jan. 2012, pp.1,7.
[40] M. E. Chehaly,O. Saadeh, C. Martinez and G. Joos, "Advantages and applications of vehicle to grid mode of operation in plug-in hybrid electric vehicles", IEEE Electrical Power & Energy Conf., Montreal, QC, 22-23 Oct. 2009, pp. 1 - 6.